1977

The relationship of structure to effectiveness of some organophosphorus insecticides and the crystal and molecular structures of tris (bicarbonato)tetraaquoholmium (III) dihydrate and tris(ethylenediamine)-cobalt(III) tetrakis (isothiocyanato)-cobaltate(II) nitrate

Wayne Joseph Rohrbaugh
Iowa State University

INFORMATION TO USERS

This material was produced from a microfilm copy of the original document. While the most advanced technological means to photograph and reproduce this document have been used, the quality is heavily dependent upon the quality of the original submitted.

The following explanation of techniques is provided to help you understand markings or patterns which may appear on this reproduction.

1. The sign or "target" for pages apparently lacking from the document photographed is "Missing Page(s)". If it was possible to obtain the missing page(s) or section, they are spliced into the film along with adjacent pages. This may have necessitated cutting thru an image and duplicating adjacent pages to insure you complete continuity.

2. When an image on the film is obliterated with a large round black mark, it is an indication that the photographer suspected that the copy may have moved during exposure and thus cause a blurred image. You will find a good image of the page in the adjacent frame.

3. When a map, drawing or chart, etc., was part of the material being photographed the photographer followed a definite method in "sectioning" the material. It is customary to begin photoing at the upper left hand corner of a large sheet and to continue photoing from left to right in equal sections with a small overlap. If necessary, sectioning is continued again — beginning below the first row and continuing on until complete.

4. The majority of users indicate that the textual content is of greatest value, however, a somewhat higher quality reproduction could be made from "photographs" if essential to the understanding of the dissertation. Silver prints of "photographs" may be ordered at additional charge by writing the Order Department, giving the catalog number, title, author and specific pages you wish reproduced.

5. PLEASE NOTE: Some pages may have indistinct print. Filmed as received.

University Microfilms International
300 North Zeeb Road
Ann Arbor, Michigan 48106 USA
St. John's Road, Tyler's Green
High Wycombe, Bucks, England HP10 8HR

The relationship of structure to effectiveness of some organophosphorus insecticides and the crystal and molecular structures of tris(bicarbonato)tetraaquoholmium (III) dihydrate and tris(ethylenediamine)-cobalt(III) tetrakis (isothiocyanato)-cobaltate(II) nitrate

by

Wayne Joseph Rohrbaugh

A Dissertation Submitted to the
Graduate Faculty in Partial Fulfillment of
The Requirements for the Degree of
DOCTOR OF PHILOSOPHY

Department: Chemistry
Major: Physical Chemistry

Approved:

Signature was redacted for privacy.

In Charge of Major Work

Signature was redacted for privacy.

For the Major Department

Signature was redacted for privacy.

For the Graduate College

Iowa State University
Ames, Iowa

1977

TABLE OF CONTENTS

INTRODUCTION TO ORGANOPHOSPHORUS INSECTICIDES

Acetylcholinesterase (AChE), one of the hydrolytic enzymes for acetylcholine, is the target of organophosphorus esters, including insecticides and nerve gases. Inhibition of the enzyme disturbs the normal nervous function, which results in the death of the animals in many instances. The nerve cell (neuron) consists of an elongated axon and short branched dendrites. The axon ending connects with another neuron through a synapse, or with a muscular fiber through a neuromuscular junction. The axon is covered with a membrane which has a selective permeability to ions and which is polarized at the equilibrium potential while resting. When the nerve is excited, the membrane depolarizes and the potential reverses rapidly relative to the resting potential. This is brought about by a change in ion permeability through the membrane.

The electric nerve impulse produced cannot propagate across the synaptic cleft (200 to 300 Å in interneuron synapses and 500 to 600 Å in neuromuscular junctions) between cells, but it causes the release of a chemical transmitter or neurohormone from the axon ending. The transmitter migrates to a receptor on the postsynaptic membrane of another neuron or muscle fiber. The interaction of the transmitter with the receptor causes a change in the cation conductance of the postsynaptic membrane, followed by the depolarization of the membrane. This produces the excitatory postsynaptic or end-plate potential. When the potential achieves a threshold, an action potential rises rapidly to excite the neuron or muscle fiber. The best known transmitters are acetylcholine

and noradrenaline.

Acetylcholine is synthesized in the nerve ending and stored in synaptic vesicles. The vesicles burst spontaneously and, by the stimulation of the action current, the release of acetylcholine increases quickly by 100- to 1000- fold. This causes synapse or end-plate potential (10 to 20 mv), and, consequently, the excitation of the postsynaptic membrane. The released acetylcholine is then rapidly hydrolyzed by AChE into inactive acetic acid and choline before the second impulse arrives. Most AChE in the end-plates of mammals is located near the receptors on the postsynaptic membrane. As long as there is acetylcholine present in the region of the synaptic cleft, the original state of the postsynaptic membrane cannot be reestablished. Therefore, inhibition of AChE results in the disturbance of the nervous function which leads to severe and often lethal damage in the organism.

The inhibition is the result of phosphorylation of an active enzyme site which is then unable to bind the natural substrate, i.e.

$$(RO)_2POX + EH \rightarrow (RO)_2POE + HX$$

where X is the "leaving group" on the ester and EH is the uninhibited AChE.[1] This phosphorylation is due, in part, to the chemical and structural similarities between acetylcholine and the many OP insecticides. The phosphate ester plays the role of the acetyl group and binds to the esteratic site of AChE. Some portion of the leaving group corresponds to the quaternary nitrogen of acetylcholine and binds to the anionic site of AChE. The phosphorylated enzyme is very stable and thus the concentration of AChE available for hydrolyzing acetylcholine decreases. Determining

the relationship of structure to effectiveness of organophosphorus insecticides, then, requires a close examination of structural parameters to develop models for AChE enzyme surfaces and to determine the nature of the active sites.

THE CRYSTAL AND MOLECULAR STRUCTURE OF AZINPHOS-METHYL

Introduction

As discussed by Baughman and Jacobson,[2] accurate three-dimensional structural analyses of organophosphorus insecticides can provide useful information toward the elucidation of bioactive mechanisms. In the first of this series of structural investigations of organophosphorus insecticides, ronnel (O,O-dimethyl O-2,4,5-trichlorophenyl phosphorothioate) was studied and characterized. From that structural analysis it was found that the distance from the phosphorus to the meta-hydrogen on the phenyl ring was 5.51 Å. When the autotoxicosis through inhibition of acetylcholinesterase (AChE) by organophosphorus insecticides is considered, it is interesting to note that the nitrogen to carbonyl carbon atom distance in acetylcholine is estimated at 4.7 Å,[3] when the molecule is in a proper conformation to react with bovine erythrocyte AChE. From a series of experiments carried out by Hollingworth et al., however, it was concluded that the distance between the anionic and esteratic centers of fly head AChE may be as much as 1 Å greater than in the mammalian enzyme.[4] Consequently, the distance between the phosphorus and an electron-deficient site in an effective organophosphorus insecticide would appear to be between approximately 4.7 and 5.7 Å.

The ubiquitous or specific effectiveness of a particular organophosphorus insecticide may depend, then, on its ability to accommodate a range of esteratic-anionic site distances in various AChE enzymes. In some

organophosphorus insecticides, the range of phosphorus to positive center distances attainable by the molecule is limited by a single rotational degree of freedom for phosphorus about the aryl ring system. For example, in ronnel, the phosphorus-(meta-hydrogen) distance is limited by rotation of phosphorus about the C(1)-O(1) bond.[2] This limitation is reflected in a comparison of ronnel's LD_{50} for a particular AChE enzyme with the LD_{50}'s of other organophosphorus insecticides, assuming that the in vivo transport properties are similar and that the inhibition of AChE is the primary toxic mode.

For ronnel, the LD_{50} in female rats is 1740 mg/kg, whereas for azinphos-methyl it is 16.[5] This implies that azinphos-methyl, or more likely its P=O metabolite, is approximately 100 times more efficient than ronnel or its corresponding metabolite in the inhibition of rat AChE. It therefore becomes interesting to investigate the charge separation distance and steric hindrances in azinphos-methyl and to compare them to ronnel. Consequently, a single crystal X-ray diffraction investigation of azinphos-methyl (O,O-dimethyl S-(4-oxo-1,2,3-benzotriazin-3-yl)-methyl phosphorodithioate) was carried out.

Experimental

Crystal Data A sample of the title compound was kindly supplied by P. A. Dahm. A crystal of dimensions 0.2 x 0.2 x 0.3 mm was mounted on a glass fiber with Duco cement and subsequently attached to a standard goniometer head. From six preliminary ω-oscillation photographs taken on an automated four-circle X-ray diffractometer at various χ and ϕ

settings, fourteen independent reflections were selected and their coordinates were input to the automatic indexing program ALICE.[6]

The resulting reduced cell and reduced cell scalars indicated 2/m (monoclinic) symmetry. A monoclinic crystal system was confirmed by inspection of axial ω-oscillation photographs, which displayed a mirror plane with respect to the b* reciprocal lattice axis. Observed layer line spacings were within experimental error to those predicted for this cell. A least-squares refinement of the lattice constants[7] based on the $\pm 2\theta$ measurements of 12 strong independent reflections on a previously aligned four-circle diffractometer (Mo Kα graphite monochromated radiation, λ = 0.70954 Å), at 10°C, yielded $\underline{a}$ = 12.084 ±0.007, $\underline{b}$ = 15.190 ±0.008, $\underline{c}$ = 7.856 ±0.003 Å, and β = 98.39 ±0.03°.

Collection and Reduction of X-ray Intensity Data Data were collected at 10°C by bathing the crystal in a cool nitrogen gas stream and by utilizing an automated four-circle diffractometer both designed and built in this laboratory. The diffractometer is interfaced to a PDP-15 computer in a time-sharing mode and is equipped with a scintillation counter. Graphite monochromated Mo Kα X-radiation was used for data collection.

All data within a 2θ sphere of 42° ($(\sin\theta)/\lambda$ = 0.500 $Å^{-1}$) in the $hk\ell$ and $\bar{h}k\ell$ octants were measured via a peak-height data collection mode, using a take-off angle of 4.5° and yielded 2751 reflections.

As a general check on electronic and crystal stability, the intensities of three standard reflections were remeasured every fifty reflections. These standard reflections were not observed to vary

significantly throughout the entire data collection period. Examination of the data revealed systematic absences of h0ℓ reflections for ℓ=2n+1 and 0k0 reflections for k=2n+1, thus uniquely defining the space group as $P2_1/c$.

The intensity data were corrected for Lorentz-polarization effects and no absorption correction was made - the crystal was nearly cylindrical and the minimum and maximum transmission factors differed by less than 5% ($\mu R = .05$). The estimated variance in each intensity was calculated by

$$\sigma_I^2 = C_T + 2C_B + (0.03\ C_T)^2 + (0.03\ C_B)^2$$

where C_T and C_B represent the total count and background count, respectively, and the factor 0.03 represents an estimate of non-statistical errors. The estimated deviations in the structure factors were calculated by the finite-difference method.[8] Equivalent zone data were averaged and only those reflections for which $F_o > 3\sigma_{(Fo)}$ were retained for structural refinement. There were consequently 696 independent reflections used in the subsequent structural analysis.

Solution and Refinement

The program MULTAN[9] was used to assign phases to the 400 largest |E| values. The E-map[10] resulting from the solution set corresponding to the best figure of merit unambiguously revealed the positions of all 19 non-hydrogen atoms. The remaining atoms were found by successive structure factor[11] and electron density map calculations.

In addition to positional parameters for all atoms, the anisotropic

thermal parameters for all non-hydrogen atoms were refined by a full-matrix least squares procedure,[11] minimizing the function $\Sigma\omega(|Fo| - |Fc|)^2$, where $\omega = 1/\sigma_F^2$, to a conventional discrepancy factor of $R = \Sigma||Fo| - |Fc||/\Sigma|Fo| = 0.091$. Analysis of the weights (ω) was performed via a requirement that $\omega(|Fo| - |Fc|)^2$ should be a constant function of $|Fo|$ and $(\sin\theta)/\lambda$.[12] Accordingly, analysis of the weighting scheme indicated that the reflections at very low as well as very high $(\sin\theta)/\lambda$ values were somewhat overweighted, and the weights were subsequently adjusted. No extinction effects were noted. Successive iterations of refinement produced convergence to R = 0.080. The scattering factors used were those of Hanson et al.,[13] modified for the real and imaginary parts of anomalous dispersion.[14]

The final positional and thermal parameters are listed in Table 1. The standard deviations were calculated from the inverse matrix of the final least-squares cycle. A listing of observed and calculated structure factor amplitudes is provided in Table 2.

Description and Discussion

A stereographic view of azinphos-methyl depicting 50% probability ellipsoids is provided in Figure 1.[15] Selected interatomic distances and angles[16] are listed in Tables 3 and 4, respectively. Intramolecular bond distances and angles are in good agreement with those reported previously in the literature.

When considering the proposal of Clark et al.[17] relating effectiveness in phosphorylation to weakness of P-(aryl-Group VIA element) bonds, azinphos-methyl should pose no problem to phosphorylation, since a

Table 1. Final atom positional[a] and thermal[b] parameters

Atom	x	y	z	β_{11}	β_{22}	β_{33}	β_{12}	β_{13}	β_{23}
S1	8051(4)[c]	7947(3)	831(6)	87(4)	43(2)	198(9)	-4(3)	17(5)	-6(4)
S2	5952(5)	8680(4)	2537(6)	92(5)	84(4)	210(11)	11(4)	32(6)	13(5)
P	7135(4)	9043(3)	1350(6)	77(4)	51(3)	166(9)	-6(3)	-5(5)	1(5)
O1	10226(11)	6905(9)	915(17)	101(13)	41(7)	290(32)	-10(8)	-19(15)	-15(11)
O2	6825(10)	9572(8)	-390(14)	115(14)	66(7)	172(25)	2(8)	-18(15)	15(12)
O3	7981(10)	9754(7)	2201(14)	108(13)	45(7)	186(27)	2(7)	-13(15)	-5(10)
N1	11623(17)	9271(11)	2472(22)	117(19)	43(11)	260(40)	-2(12)	61(23)	-11(15)
N2	10702(16)	9220(11)	1529(21)	103(17)	59(11)	184(30)	-6(12)	27(19)	18(15)
N3	10259(14)	8382(10)	1030(18)	70(13)	49(11)	162(27)	1(10)	3(15)	-9(13)
C1	11752(16)	7659(13)	2655(20)	95(19)	47(12)	142(32)	12(13)	31(22)	29(16)
C2	12341(19)	6885(15)	3306(23)	103(22)	65(14)	173(37)	-13(14)	75(25)	-1(18)
C3	13358(20)	6987(19)	4384(25)	100(22)	94(19)	197(42)	43(18)	22(25)	27(22)
C4	13787(19)	7839(18)	4808(23)	76(19)	75(16)	199(38)	-16(16)	44(20)	-21(23)
C5	13198(19)	8557(16)	4159(29)	97(23)	48(12)	267(46)	-11(14)	-3(28)	-10(21)
C6	12183(17)	8492(14)	3083(23)	89(20)	54(14)	162(35)	-15(13)	56(23)	-47(18)
C7	10690(16)	7567(14)	1432(20)	73(17)	40(11)	123(32)	26(12)	61(20)	26(16)
C8	9181(20)	8471(17)	-207(23)	115(23)	83(16)	93(40)	7(13)	-10(23)	-4(17)
C9	6134(42)	9204(28)	-1887(52)	152(39)	85(31)	243(58)	-5(23)	-6(37)	-20(32)
C10	8555(23)	9646(19)	3987(32)	120(26)	73(17)	243(61)	-23(18)	14(29)	27(23)
H1	185(16)	637(12)	312(21)						
H2	377(15)	638(12)	439(20)						
H3	471(15)	792(11)	488(19)						
H4	351(15)	911(14)	467(22)						
H5	925(24)	819(15)	1109(30)						
H6	910(13)	823(10)	873(20)						
H7	585(33)	888(25)	-148(49)						
H8	629(13)	815(11)	-204(20)						
H9	514(14)	904(11)	-128(19)						
H10	890(18)	926(14)	408(29)						
H11	782(16)	937(12)	480(23)						
H12	930(14)	1022(11)	430(19)						

[a] The positional parameters for all non-hydrogen atoms are presented in fractional unit cell coordinates (x 10^4). Positional parameters for hydrogen atoms are (x 10^3).

[b] The β_{ij} are defined by: $T = \exp\{-(h^2\beta_{11} + k^2\beta_{22} + l^2\beta_{33} + 2hk\beta_{12} + 2hl\beta_{13} + 2kl\beta_{23})\}$ For all hydrogen atoms an isotropic thermal parameter of 2.5 was assigned.

[c] In this and succeeding tables, estimated standard deviations are given in parentheses for the least significant figures.

Table 2. Observed and calculated structure factor amplitudes

L = 0			
H	K	FO	FC
0	2	70	-69
0	4	54	-49
0	8	36	-31
0	10	17	17
0	12	11	-9
1	0	71	63
1	2	42	-37
1	3	108	-94
1	4	54	54
1	5	40	-35
1	6	14	17
1	8	38	-36
1	11	49	-45
1	12	16	14
2	0	112	-101
2	1	30	31
2	2	24	-30
2	3	99	99
2	4	25	-23
2	6	19	18
2	7	54	-54
2	8	12	11
2	10	31	-27
2	11	29	-28
2	12	16	14
3	0	34	38
3	3	27	-24
3	4	67	-66
3	5	83	84
3	9	35	-35
3	12	13	14
3	13	17	15
3	14	14	-11
4	0	23	-21
4	1	56	60
4	2	20	-17
4	3	34	-37
4	5	15	-15
4	6	27	25
4	7	27	27
4	8	21	-19
4	10	22	21
4	11	22	20
4	13	18	-14
5	0	70	71
5	2	53	-58
5	4	13	15
5	6	41	40
5	7	28	29
5	12	26	-24
6	0	11	10
6	1	24	24
6	3	19	18
6	4	39	41
6	6	9	7
6	8	24	-26
6	11	16	-15
6	13	23	17
7	0	13	-12
7	1	23	25
7	2	30	30
7	3	19	22
7	4	33	-35
7	5	28	-32
7	6	12	-14
7	7	16	-14
7	8	12	9
7	11	17	-17
8	0	44	-42
8	1	12	-12
8	3	28	-31
8	5	14	12
8	7	27	26
8	11	10	-5
9	0	25	-25
9	1	42	40
9	6	31	29
10	0	35	36
10	4	13	-13
10	5	22	-21
11	1	17	-14
11	3	10	-9
L = 1			
H	K	FO	FC
-11	6	22	23
-10	1	13	11
-10	2	12	12
-9	2	39	-40
-9	5	15	15
-8	1	37	-37
-8	2	17	-16
-8	3	30	29
-8	4	12	13
-8	6	14	-15
-8	9	14	-15
-7	1	13	12
-7	2	30	32
-7	5	49	-49
-7	7	24	24
-7	8	13	-12
-6	2	22	-23
-6	4	38	-18
-6	5	15	-20
-6	6	58	59
-6	7	13	-15
-6	8	13	-9
-5	1	33	-36
-5	2	24	23
-5	4	29	-30
-5	5	31	32
-5	7	15	14
-5	8	27	26
-5	10	23	25
-4	1	46	46
-4	4	55	55
-4	5	27	26
-4	6	28	-28
-4	7	17	18
-4	8	19	21
-4	10	12	-10
-4	11	16	-16
-4	14	16	15
-3	1	67	65
-3	2	35	-37
-3	3	63	67
-3	4	28	-28
-3	5	34	-35
-3	6	63	-66
-3	7	39	-38
-3	8	15	14
-3	9	13	-12
-3	11	28	27
-2	2	54	-62
-2	3	36	-38
-2	4	85	-90
-2	5	85	-94
-2	6	15	-16
-2	7	61	59
-2	8	14	16
-2	9	15	-16
-2	11	16	-19
-2	13	30	34
-2	14	16	-16
-1	1	42	-47
-1	2	76	85
-1	3	26	-31
-1	4	32	25
-1	5	21	-17
-1	6	60	66
-1	8	27	-31
-1	9	22	-26
-1	11	19	-20
-1	13	33	34
-1	14	11	10
0	1	101	81
0	2	150	145
0	4	34	34
0	7	35	-34
0	10	23	25
0	11	14	11
0	12	11	-11
0	14	16	14
1	1	47	41
1	2	90	-76
1	3	65	-61
1	4	51	49
1	5	27	28
1	6	28	27
1	7	16	14
1	8	14	11
1	9	24	27
1	10	19	-22
2	1	53	-54
2	3	74	59
2	4	57	53
2	5	13	18
2	6	25	-24
2	7	41	41
2	8	23	23
2	9	29	-29
2	12	18	-17
3	3	21	20
3	4	29	30
3	5	46	-45
3	6	63	-59
3	7	69	61
3	8	18	-14
3	9	26	-23
3	11	27	-23
4	1	13	-10
4	2	24	-24
4	4	30	-30
4	5	36	-36
4	6	24	25
4	7	24	-24
4	8	28	-25
4	11	20	19
5	2	18	19
5	3	14	-16
5	4	26	-26
5	5	16	17
5	8	33	28
5	10	27	24
5	12	17	-17
6	1	10	-9
6	4	35	34
6	5	49	48
6	10	15	-12
7	1	15	-12
7	3	23	23
7	4	15	15
7	6	38	-37
7	11	18	15
8	2	22	-20
8	3	11	-10
8	5	41	-40
8	7	31	32
8	8	29	29
9	1	20	-21
9	5	20	19
9	8	16	15
10	1	12	9
10	2	29	28
11	2	12	-14
11	3	11	-8
L = 2			
H	K	FO	FC
-12	0	16	-16
-11	1	13	7
-11	2	10	-8
-11	6	22	18
-9	0	44	45
-9	1	22	-26
-9	4	12	-12
-9	9	18	15
-8	0	10	10
-8	1	45	-47
-8	2	18	-17
-8	4	16	18
-8	6	21	21
-7	0	23	-22
-7	1	30	32
-7	2	20	19
-7	3	32	30
-7	6	15	14
-7	7	21	-22
-6	0	53	51
-6	3	34	-34
-6	4	51	-53
-6	5	28	-28
-6	8	10	10
-6	9	22	-23
-5	0	45	-42
-5	1	19	18
-5	2	60	-64
-5	3	49	-51
-5	4	34	35
-5	5	29	-26
-5	7	41	44
-5	8	23	-23
-5	10	15	18
-5	13	15	-17
-4	0	73	68
-4	1	23	21
-4	2	34	-39
-4	3	59	62
-4	4	14	15
-4	9	17	19
-4	12	12	-10
-3	0	260	214
-3	1	47	-55
-3	3	26	31
-3	5	13	16
-3	8	15	-15
-3	11	22	-22
-3	12	15	13
-3	13	33	34
-2	0	52	59
-2	1	155	154
-2	4	13	-12
-2	5	49	-44
-2	11	28	-29
-2	12	29	28
-2	13	14	-13
-1	0	75	-69
-1	1	116	103
-1	2	51	48
-1	3	27	-30
-1	4	29	-30
-1	5	27	30
-1	6	17	22
-1	7	22	26
-1	8	16	18
-1	9	27	-27
-1	10	33	-35
0	0	42	-32
0	1	70	53
0	2	53	-48
0	3	17	-15
0	4	44	43
0	6	28	28
0	7	22	-21
0	8	36	-35
0	9	38	-40
0	10	12	14
0	11	16	14
0	13	12	12
1	0	127	109
1	1	71	63
1	2	72	-64
1	4	84	-77
1	5	29	-25
1	6	34	33
1	10	35	38
1	12	11	-12
2	0	27	-23
2	1	91	-85
2	3	39	-34
2	4	22	22
2	6	22	21
2	7	63	59
2	9	22	25
2	11	20	-21
3	0	63	-66
3	1	58	56
3	2	21	22
3	3	31	28
3	4	45	39
3	5	33	-31
3	6	21	20
3	7	17	-16
3	10	29	-30
4	0	33	-33
4	1	60	58
4	2	43	40
4	3	16	-16
4	4	59	-61
4	6	23	-26
4	8	19	21
4	9	39	-40
5	0	71	-69
5	1	10	13
5	3	27	-29
5	4	18	19
5	6	19	-19
5	7	42	43
5	8	20	-18
5	10	27	26
6	0	19	20
6	2	15	-16
6	4	19	17
6	6	33	31
6	7	19	19
6	12	31	-31
7	3	12	12
7	5	25	-27
7	9	17	-14
8	0	11	-12
8	5	34	-35
8	6	34	-32
8	8	15	16
8	9	15	14
9	0	11	-9
9	3	24	-25
10	0	19	-17
10	1	18	19
10	4	15	13
11	0	19	19
11	1	17	15
L = 3			
H	K	FO	FC
-9	7	24	-23
-9	9	13	8
-8	2	21	-19
-8	3	18	-16
-8	7	12	15
-8	8	25	28
-7	1	18	-13
-7	2	9	-7
-7	3	44	40
-7	4	34	32
-7	6	13	-13
-7	8	15	16
-6	1	33	32
-6	2	33	32
-6	3	19	18
-6	4	18	-21
-6	5	24	-28
-6	6	27	-29
-5	1	13	15
-5	2	23	-30
-5	3	11	-13
-5	4	34	-39
-5	5	19	-22
-5	6	39	45
-5	8	10	-10
-4	2	39	42
-4	5	26	31
-4	7	23	-30
-4	8	13	13
-4	11	17	-17
-4	12	21	-16
-3	1	19	19
-3	2	43	44
-3	3	35	-41
-3	4	47	51
-3	6	40	-46
-2	1	38	-34
-2	3	24	27
-2	4	38	45
-2	5	12	-18
-2	6	11	-10
-2	8	16	16
-2	10	15	-17
-2	11	31	35
-1	3	14	10
-1	4	29	-27
-1	5	19	-20
-1	7	52	59
-1	8	23	24
-1	9	13	-13
-1	10	13	13
-1	11	14	-13
-1	14	14	-14
0	1	46	-41
0	2	13	-12
0	4	14	-16
0	5	24	24
0	7	36	35
0	8	28	-31
0	9	20	-18
0	10	12	-12
0	11	22	-22
1	2	41	41
1	3	47	-42
1	5	16	14
1	6	37	-36
1	7	54	-55
1	9	20	20
1	11	17	17
2	1	44	47
2	2	62	-56
2	3	38	-33
2	4	20	18
2	6	16	14
2	8	40	41
2	9	17	18
3	1	27	-28
3	2	28	-32
3	3	71	70
3	4	27	23
3	5	39	37
3	6	27	-28
3	8	19	18
3	9	20	-21
3	13	12	-9
4	1	18	-14
4	2	18	20
4	3	15	13
4	4	12	-7
4	5	19	-17
4	6	34	-34
4	7	21	19
4	8	28	-25
5	2	25	-25
5	4	15	-13
5	5	26	-30
5	6	31	31
5	11	14	13
6	4	16	-16
6	5	29	28
6	6	12	-10
6	7	30	-31
6	8	28	31
6	10	13	14
7	3	12	-13
7	4	11	9
7	5	25	26
7	7	16	-18
8	3	21	22
8	4	22	22
9	1	20	20
9	5	15	-15
10	1	14	-14
L = 4			
H	K	FO	FC
-10	1	26	24
-10	2	9	-5
-9	0	14	11
-8	0	15	16
-8	2	21	-19
-8	5	23	-23
-8	9	16	14
-7	1	20	-21
-6	0	19	-18
-6	1	17	20
-6	2	14	12
-6	3	21	23
-6	4	14	15
-6	7	16	-17
-6	10	12	-10
-5	0	77	68
-5	1	77	83
-5	4	28	-35
-5	5	9	5
-5	8	15	16
-4	0	50	-50
-4	1	53	53
-4	2	15	12
-4	3	40	-45
-4	4	28	29
-4	7	26	29
-4	8	14	-15
-4	11	14	-10
-3	0	65	-58
-3	1	16	12
-3	2	17	-17
-3	3	36	39
-3	4	19	19
-3	5	21	-22
-3	6	22	26
-3	7	26	-28
-3	11	12	-9
-3	12	27	-26
-2	0	30	25
-2	1	23	-25
-2	3	14	15
-2	4	43	-43
-1	0	55	-48
-1	2	64	59
-1	3	22	-20
-1	5	33	-36
-1	7	31	38
-1	9	21	23
-1	12	14	14
0	0	12	-11
0	1	28	24
0	2	18	16
0	3	38	-35
0	6	18	15
0	10	27	-26
0	11	11	8
1	0	51	-51
1	1	37	36
1	2	19	-15
1	3	24	-21
1	5	10	11
1	6	18	-17
1	9	36	-37
1	10	18	18
2	0	13	-13
2	3	34	31
2	4	19	-17
2	6	22	-22
2	9	18	20
2	10	18	23
3	1	69	-72
3	3	11	-14
3	4	10	10
3	5	17	16
3	7	23	24
4	0	50	-59
4	2	23	22
4	4	25	23
4	5	23	-22
4	10	16	-18
5	0	15	16
5	1	23	21
5	2	30	32
5	3	13	11
5	4	11	-11
5	6	31	-34
5	8	23	25
5	9	14	-15
6	3	39	-39
6	4	19	22
6	6	35	-35
7	2	22	-25
8	3	25	24
9	2	17	21
L = 5			
H	K	FO	FC
-9	1	12	9
-8	5	11	5
-8	7	29	-29
-7	6	16	-13
-7	8	16	17
-6	1	25	-25
-6	4	17	18
-6	7	14	13
-5	2	44	46
-5	3	16	16
-5	6	11	-9
-4	2	25	-20
-4	4	30	-29
-4	6	24	27
-4	9	12	11
-3	1	38	-35
-3	4	16	-16
-3	5	38	40
-3	6	16	-17
-2	2	18	12
-2	3	38	-38
-2	4	28	31
-2	6	42	-41
-2	9	11	9
-1	1	10	16
-1	2	77	-76
-1	3	18	13
-1	4	18	19
-1	5	19	-19
-1	6	13	17
-1	8	17	19
0	3	32	32
0	4	27	-25
0	7	17	15
1	2	11	-11
1	5	21	22
1	6	14	16
1	8	24	-26
2	7	32	-34
2	8	17	-17
3	1	18	22
3	2	37	-38
3	3	29	-27
3	6	25	-23
3	7	13	-12
3	8	72	22
3	9	15	12
4	1	34	-36
4	2	17	-18
4	3	12	11
4	5	16	16
5	2	39	40
5	4	14	13
5	5	15	-12
5	6	12	10
5	8	18	-18
6	1	22	26
6	5	13	-14
6	6	16	16
7	4	13	-12
7	5	21	22
L = 6			
H	K	FO	FC
-8	0	23	22
-7	0	20	-20
-7	1	15	18
-7	4	12	7
-6	0	51	-51
-6	1	20	-17
-6	2	14	13
-5	0	39	-38
-5	3	14	12
-4	0	28	29
-4	1	27	26
-4	2	18	19
-4	4	16	-17
-4	5	17	-17
-4	7	16	15
-3	1	15	-16
-3	3	30	-31
-3	4	18	16
-3	7	15	15
-2	0	19	-20
-2	2	17	-17
-2	3	19	19
-2	4	20	19
-2	7	16	-18
-1	1	20	-22
-1	2	16	16
-1	3	24	22
-1	4	32	-32
0	0	29	-28
0	1	38	-37
0	2	15	13
0	3	18	-13
0	6	15	-14
0	7	16	13
1	6	16	15
1	7	12	12
2	0	21	24
2	6	17	-16
3	0	23	22
3	1	13	-13
3	4	14	13
3	6	26	-29
3	7	20	-20
4	1	24	-26
4	3	13	-8
4	5	19	10
5	0	29	-32
5	3	14	13
6	1	14	14
L = 7			
H	K	FO	FC
-5	1	15	-12
-4	2	20	20
-3	1	19	17
-3	4	18	-18
-2	1	12	-10
-2	2	11	-10
-2	5	30	27
-1	1	17	17
-1	4	18	17
-1	6	20	-21
0	2	29	-29
0	5	23	-23
1	1	14	-15
2	2	13	13

Figure 1. Stereographic view of azinphos-methyl with hydrogen atoms omitted
In this and succeeding drawings 50% probability ellipsoids are depicted

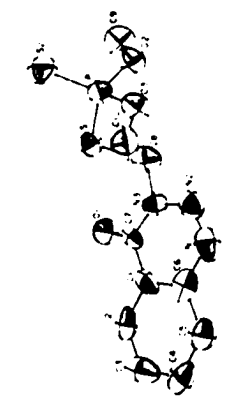

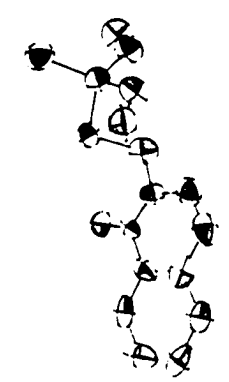

Table 3. Selected interatomic distances (Å) for azinphos-methyl

P-S1	2.071(7)
P-S2	1.898(7)
P-O2	1.580(12)
P-O3	1.565(12)
S1-C8	1.863(28)
O1-C7	1.191(20)
O2-C9	1.448(30)
O3-C10	1.478(26)
N1-N2	1.243(20)
N1-C6	1.408(25)
N2-N3	1.410(22)
N3-C7	1.360(21)
N3-C8	1.510(28)
C1-C2	1.426(26)
C1-C6	1.388(25)
C1-C7	1.490(24)
C2-C3	1.393(28)
C3-C4	1.412(31)
C4-C5	1.357(28)
C5-C6	1.385(27)

Table 4. Bond angles (deg) for azinphos-methyl

P-S1-C8	100.9(8)	C6-C1-C2	120.8(18)
S1-P-S2	109.0(3)	C7-C1-C2	119.3(18)
S1-P-O2	107.7(6)	C7-C1-C6	119.8(18)
S1-P-O3	107.7(5)	C1-C2-C3	118.3(22)
S2-P-O2	118.1(6)	C2-C3-C4	120.3(22)
S2-P-O3	118.7(5)	C3-C4-C5	119.4(19)
O2-P-O3	94.3(7)	C4-C5-C6	122.6(20)
P-O2-C9	122.6(20)	C5-C6-C1	118.6(21)
P-O3-C10	120.9(12)	C5-C6-N1	119.0(19)
C6-N1-N2	119.5(16)	C1-C6-N1	122.4(16)
N1-N2-N3	119.4(15)	O1-C7-C1	128.0(16)
N2-N3-C7	129.6(15)	N3-C7-O1	122.8(17)
N2-N3-C8	110.7(15)	N3-C7-C1	109.1(18)
C7-N3-C8	119.6(20)	S1-C8-N3	107.3(13)

phosphorus-sulfur bond is certainly a weaker bond than an analogous P-O bond commonly found in organophosphorus insecticides. Consequently, the inhibition of AChE by azinphos-methyl oxon should not be hindered by any significant barrier to phosphorylation. Distortion of tetrahedral geometry about phosphorus is observed in this compound as in others previously reported.[18] The (methoxy-oxygen)-phosphorus-(methoxy-oxygen) angle, in particular, is nearly 4 degrees smaller than that reported for ronnel,[2] i.e. 94.3(7) to 98.0(3)°, respectively.

The planarity of the ring system is quite striking, as can be seen in the tabulation of atom deviations from the least-squares plane (Table 5). The greatest deviation from planarity is ~0.03 Å, which is negligible when considering thermal motion and standard deviations.

Packing forces do not appear to dictate coordination geometry about the phosphorus atom to any great extent, but torsion angles do appear to be affected by intermolecular steric repulsion effects of the methoxy groups (cf. Figure 2). Torsion angles about specific bonds are listed in Table 6.

C7 appears to be the likely atom on which an electron deficient site may reside. The P-C7 distance in the solid state for azinphos-methyl is 4.83(2) Å. The corresponding distance for ronnel is 5.51 Å. From solid state considerations alone, the phosphorus-(partially positive center) distance in ronnel is 0.7 Å longer than the corresponding distance for azinphos-methyl. It is suggested by Hollingworth et al.[4] that the distance between anionic and esteratic sites of insect AChE may be as much as 1 Å greater than in mammalian enzymes. Thus, it would appear that

Table 5. Atomic displacements from the least-squares plane[a] describing the ring system

Plane defined by atoms (O1,N1,N2,N3,C1,C2,C3,C4,C5,C6,C7, and C8):

$$-0.61582\ X - 0.00129\ Y + 0.78789\ Z + 6.95512 = 0$$

Atom	Deviation from Planarity (Å)
O1	-0.027
N1	-0.008
N2	0.034
N3	0.024
C1	0.024
C2	0.032
C3	0.011
C4	-0.020
C5	-0.026
C6	-0.006
C7	-0.021
C8	-0.018

[a]Plane is defined as $c_1X+c_2Y+c_3Z-d = 0$, where X, Y, and Z are Cartesian coordinates related to the monoclinic x,y,z coordinates by the transformation: a,0,c cosβ; 0,b,0; 0,0,c sinβ.

Figure 2. Unit cell stereograph of azinphos-methyl

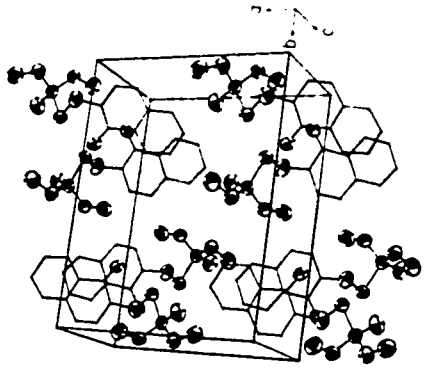

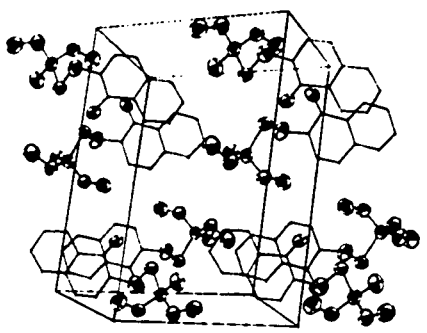

Table 6. Torsion angles

Plane A	Plane B	Bond of Rotation	Torsion Angle (∠AB) (Degrees)
S1-P-S2	C8-S1-P	S1-P	177.8
N3-C8-S1	C8-S1-P	C8-S1	107.5
N2-N3-C8	N3-C8-S1	N3-C8	117.4
Least Squares Plane for Ring	N3-C8-S1	N3-C8	64.0

azinphos-methyl oxon would be a more effective AChE inhibitor than the corresponding analog of ronnel for the mammalian enzymes, based on the work of Chothia and Pauling and Hollingworth *et al.* mentioned previously. Indeed, such an assumption is substantiated when a comparison of the LD_{50}'s in female rats for azinphos-methyl and ronnel is made, i.e. LD_{50} azinphos-methyl = 16 mg/kg, LD_{50} ronnel = 1740.[5]

It is evident that rotation about the N3-C8 and C8-S1 bonds of azinphos-methyl provide considerable flexibility for the phosphorus to C7 distance, since there are no intramolecular restrictive interactions. Azinphos-methyl oxon, therefore, is not exclusively an insect AChE inhibitor, since free rotation *in vivo* about the N3-C8 and C8-S1 bonds enable the molecule to accommodate a large range of anionic-esteratic site separations. Ronnel, on the other hand, has only a single rotational flexibility for altering the phosphorus-(meta-hydrogen) separation about the C1-O1 bond, and intramolecular repulsion effects limit the molecule in achieving separations which are more efficient for blocking of mammalian AChE.[2]

The structure of azinphos-methyl therefore suggests that the additional rotational flexibility of phosphorus relative to the positive site of the aryl ring system broadens the specificity of the insecticide. It appears that in the design of organophosphorus insecticides one should consider the range of phosphorus-(partially positive center) distances attainable as a criterion for specificity. In addition, it seems suggestive from this work that similar organophosphorus insecticides with an additional bound atom between phosphorus and the aryl ring are less

specific to insects and, consequently, may not be desirable models for insecticide development.

It is interesting to note that the phosphinate analog of azinphos-methyl has an LD_{50} for rats which is significantly larger, i.e. = 1000 mg/kg.[19] This implies that accommodation of the AChE enzyme is not dictated solely by phosphorus-(partially positive center) separations, but may also involve a subtle charge density effect about the phosphorus, consequently easing or hindering phosphorylation or enzyme binding.

Results of a CNDO II molecular orbital calculation[20] for both azinphos-methyl and its phosphinate analog support the intuitive conjecture that the charge on the phosphorus atom should differ slightly in these two compounds (cf. Figure 3). A charge density calculation for azinphos-methyl was made based on the positional parameters obtained from the structural study, and a similar calculation was performed for the phosphinate analog based on the assumption that the structural parameters should not differ significantly from those obtained for azinphos-methyl. The substitution of methyl carbon atoms in the methoxy-oxygen positions of azinphos-methyl at phosphorus-carbon distances of ~1.56 Å yields the results shown in Figure 3. In general, the phosphorus-carbon distances should be somewhat longer, and a CNDO II calculation with the methyl groups radially displaced such that the P-C distance is ~1.74 Å, yields an even lower value for the positive charge on phosphorus (+0.853), leaving all other atomic charges essentially unchanged. The numbers associated with the partial charge densities in Figure 3 are not intended to represent the absolute charge on each atom,

Figure 3. Partial charge densities obtained from CNDO II molecular orbital calculations for (a) azinphos-methyl and (b) its phosphinate analog

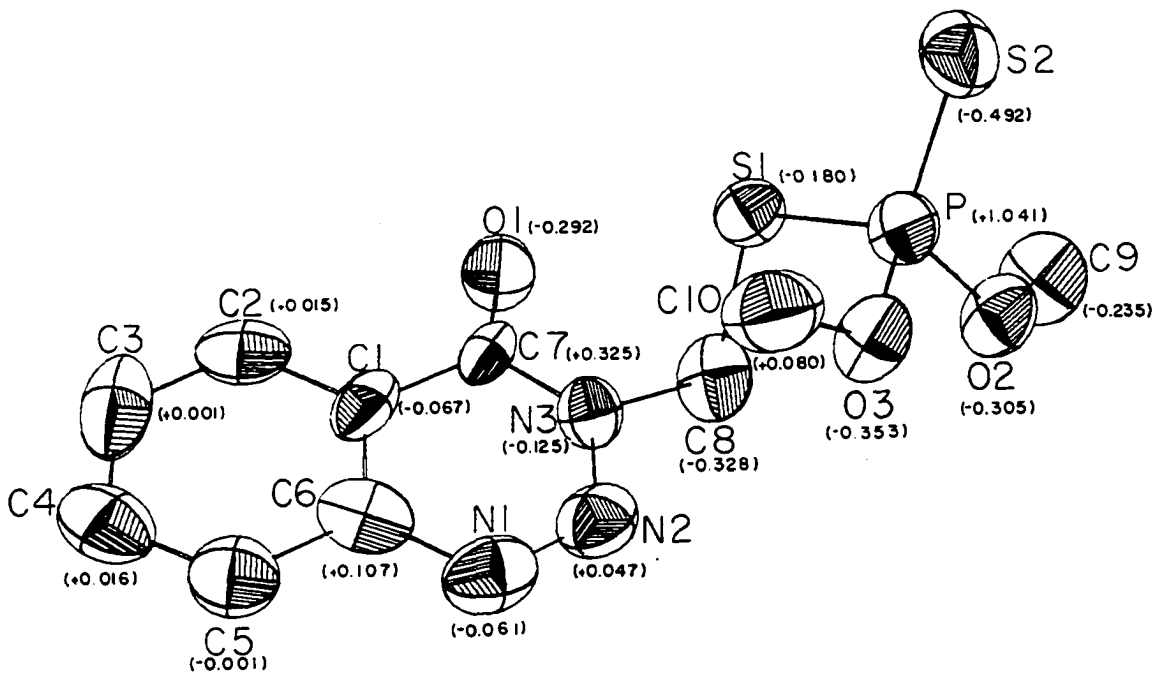
S2
(-0.492)
S1 (-0.180)
P (+1.041)
C9
(-0.235)
O1 (-0.292)
C10
C2 (+0.015)
C3
C1
C7 (+0.325)
(+0.080)
O3
O2
(-0.305)
(+0.001)
(-0.067)
N3
(-0.125)
C8
(-0.328)
(-0.353)
C4
C6
N1
N2
(+0.016)
(+0.107)
(+0.047)
C5
(-0.001)
(-0.061)

(a)

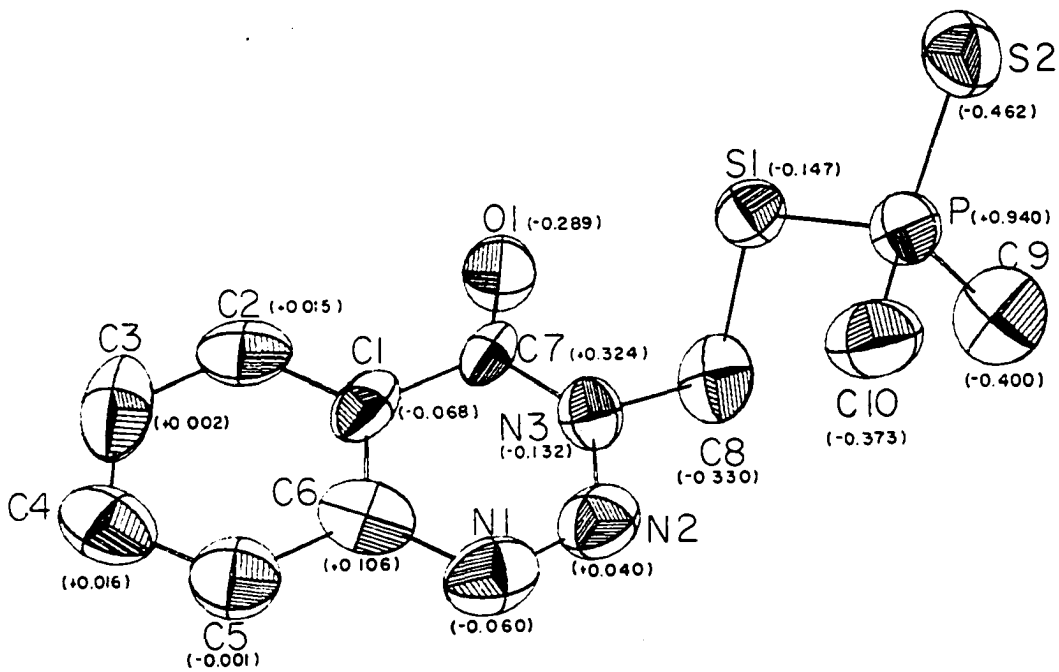
S2
(-0.462)
S1 (-0.147)
P (+0.940)
O1 (-0.289)
C9
C2 (+0.015)
C3
C1
C7 (+0.324)
(-0.400)
C10
(+0.002)
(-0.068)
N3
(-0.132)
C8
(-0.330)
(-0.373)
C4
C6
N1
N2
(+0.016)
(+0.106)
(+0.040)
C5
(-0.001)
(-0.060)

(b)

since the CNDO II calculation is an approximation of physical reality. Comparisons, however, should be valid since the same approximations are applied to both molecules.

From these calculations, it can be seen that the partial charge density on the phosphorus atom is significantly different in these two molecules, whereas, the charge on C7 remains essentially invariant. Since the toxicity of the phosphinate analog to mammals is significantly lower than that of azinphos-methyl and since the structural parameters of the two compounds would appear to be similar, it seems logical to suspect a charge density dependence in the toxic mechanism.

These results, consequently, provide impetus for future calculations of charge densities in other series of organophosphorus insecticides. In addition to the possibility of charge density effects in AChE inhibition, intramolecular restrictions or freedoms may also contribute to the inhibition, and X-ray diffraction analyses of organophosphorus insecticides can provide valuable information to elucidate the mechanisms of acetylcholinesterase inhibition in both mammals and insects.

THE CRYSTAL AND MOLECULAR STRUCTURE OF AMIDITHION

Introduction

As discussed in previous crystal structure analyses of organophosphorus insecticides,[2,18,21] the ubiquitous or specific effectiveness of a particular insecticide may depend on its ability to accommodate a range of esteratic-anionic site separations in various acetylcholinesterase (AChE) enzymes. In addition, the effectiveness may also be related to the relative charge densities on the corresponding sites of the insecticide.[21] In order to substantiate or refute these conjectures, sufficient data must be obtained for a number of organophosphorus insecticides with varying degrees of effectiveness as reflected by insect and mammalian toxicities.

The structure of azinphos-methyl,[21] with a mammalian toxicity of LD_{50} = 16 mg/kg, exhibits a solid-state esteratic-anionic site separation, as measured by the phosphorus to oxo-carbon distance, of 4.83 Å, and partial charge densities (via a CNDO calculation) of +1.041 and +0.325 e at these atoms, respectively. It was felt that it would be of interest to compare such parameters with those obtained for insecticides exhibiting less toxicity in mammalian systems in order to deduce correlations, if any, between these parameters and insecticide effectiveness. Therefore, a crystal of amidithion (O,O-dimethyl-S-(N-2-methoxyethylcarbamoylmethyl)-phosphorodithioate), $C_7H_{16}NO_4PS_2$, with an LD_{50} of 420 mg/kg,[5] was chosen for three-dimensional X-ray analysis.

Experimental

Crystal Data A sample of amidithion was kindly supplied by the Pesticides and Toxic Substances Effects Laboratory, U.S.E.P.A., Research Triangle Park, N.C. A nearly cylindrical crystal of dimensions 0.15 x 0.15 x 0.25 mm was mounted in a 0.2 mm thin-walled Lindemann glass capillary and subsequently attached to a standard goniometer head. From four preliminary ω-oscillation photographs taken on an automated four-circle X-ray diffractometer at various χ and ϕ settings, fourteen independent reflections were selected and their coordinates were input to an automatic indexing algorithm.[6]

The resulting reduced cell and reduced cell scalars indicated 2/m (monoclinic) symmetry. The monoclinic crystal system was confirmed by inspection of axial ω-oscillation photographs, which displayed a mirror plane with respect to only the b* reciprocal lattice axis. Observed layer line spacings were within experimental error to those predicted for this cell. A least-squares refinement of the lattice constants[22] based on the precise $\pm 2\theta$ measurements of 12 strong independent reflections on a previously aligned four-circle diffractometer (Mo Kα graphite-monochromated radiation, λ = 0.70954 Å), yielded a = 10.975(3), b = 9.335(2), c = 13.702(4) Å, and β = 102.84(4)°.

Collection and Reduction of X-ray Intensity Data Data were collected at room temperature on an automated four-circle diffractometer designed and built in this laboratory.[23] The diffractometer is interfaced to a PDP-15 computer in a time-sharing mode and is equipped with a scintillation counter. Graphite-monochromated Mo Kα radiation was used

for data collection.

All data (2209 reflections) within a 2θ sphere of 45° ($(\sin\theta)/\lambda$ = 0.539 $\AA^{-1}$) in the hkℓ and $\bar{h}$kℓ octants were measured via an ω-scan data collection mode, using a take-off angle of 4.5°.

As a general check on electronic and crystal stability, the intensities of three standard reflections were remeasured every 75 reflections. These standard reflections were not observed to vary significantly throughout the entire data collection period. Examination of the data revealed systematic absences of the h0ℓ reflections for ℓ=2n+1 and 0k0 reflections for k=2n+1, thus uniquely defining the space group as $P2_1/c$.

The intensity data were corrected for Lorentz-polarization effects and, since the minimum and maximum transmission factors differed by less than 5% for $\mu = 0.49$ cm^{-1}, no absorption correction was made. The estimated variance in each intensity was calculated by

$$\sigma_I^2 = C_T + 2C_B + (0.03\ C_T)^2 + (0.03\ C_B)^2$$

where C_T and C_B represent the total count and background count, respectively, and the factor 0.03 represents an estimate of non-statistical errors. The estimated deviations in the structure factors were calculated by the finite-difference method.[8] Equivalent zone data were averaged and only those reflections for which $F_o > 2\sigma_{Fo}$ were retained for structural refinement. There were consequently 1512 independent reflections used in subsequent calculations.

Solution and Refinement

The program MULTAN[9] was used to assign phases to the 300 largest $|E|$ values. The E-map[10] resulting from the solution set corresponding to the best figure of merit unambiguously revealed the positions of 12 non-hydrogen atoms. The remaining atoms were found by successive structure factor[11] and electron density map calculations. Methyl hydrogen ambiguities were resolved by refining two sets of methyl hydrogens for each methyl carbon. The sets were displaced by 60° and were each assigned half occupancy.

In addition to positional parameters for all atoms, the anisotropic thermal parameters for all non-hydrogen atoms were refined by a full-matrix least-squares procedure,[11] minimizing the function $\Sigma\omega(|Fo| - |Fc|)^2$ where $\omega = 1/\sigma_F^2$, to a conventional discrepancy factor of $R = \Sigma||Fo| - |Fc|\Sigma/|Fo| = 0.071$. Analysis of the weights (ω) was performed via a requirement that $\omega(|Fo| - |Fc|)^2$ should be a constant function of $|Fo|$ and $(\sin\theta)/\lambda$.[12] Accordingly, inspection of the weighting scheme indicated that the reflections at very low as well as very high $(\sin\theta)/\lambda$ values were somewhat overweighted, and the weights were subsequently adjusted. Seven strong, low-angle reflections exhibited secondary extinction effects and were removed from the data set. Successive iterations of refinement on the 1505 remaining reflections produced convergence to $R = 0.066$ and $R_w = 0.077$, where $R_w = [\Sigma\omega(|Fo| - |Fc|)^2/\Sigma\omega|Fo|^2]^{\frac{1}{2}}$. The scattering factors used for non-hydrogen atoms were those of Hanson *et al.*,[13] modified for the real and imaginary parts of anomalous dispersion.[14] The hydrogen scattering

factors were those of Stewart et al.[24]

The final positional and thermal parameters are listed in Table 7. The standard deviations were calculated from the inverse matrix of the final least-squares cycle. A list of observed and calculated structure factor amplitudes is provided in Table 8.

Description and Discussion

A stereographic view of amidithion depicting 50% probability ellipsoids is provided in Figure 4[15] and interatomic distances and angles[16] are listed in Table 9. Intramolecular bond distances and angles are in good agreement with those reported previously in the literature.

As has been observed in prior crystal structure analyses of organophosphorus insecticides,[2,18,21] the geometry about the phosphorus can be described as a distorted tetrahedron. In particular, the angles involving the doubly-bonded sulfur, S(1), with the methoxy oxygens are both approximately 9° greater than tetrahedral, while the (methoxy-oxygen)-phosphorus-(methoxy-oxygen) angle is reduced to 95.4(2)°. These results parallel those found in the analyses cited above and in particular are in good agreement with the results for azinphos-methyl[21] where the latter angle was found to be 94.3(7)°.

Results of a CNDO II molecular orbital calculation[20] indicate two of the most probable positive centers in addition to the phosphorus are C(2) and H (cf. Figure 5). The solid state P-C(2) and P-H distances are 3.91(1) and 4.24(2) Å, respectively. It should also be noted that

Table 7. Final atom positional[a] and thermal[b] parameters

Atom	x	y	z	β_{11}	β_{22}	β_{33}	β_{12}	β_{13}	β_{23}
S1	3568(2)[c]	6872(2)	5143(1)	161(2)	248(3)	126(1)	-49(2)	81(1)	-61(2)
S2	2362(1)	5397(1)	6835(1)	140(2)	108(2)	143(1)	15(1)	62(1)	-2(1)
P	2676(1)	7277(1)	6159(1)	95(1)	126(2)	80(1)	-9(1)	24(1)	-14(1)
OMe1	1399(3)	8084(4)	5847(3)	121(4)	215(6)	87(3)	36(4)	22(3)	18(3)
OMe2	3277(3)	6362(4)	6996(3)	118(4)	169(5)	99(3)	-26(4)	23(3)	-33(3)
OMe3	-2554(4)	8192(4)	5839(3)	177(5)	126(5)	96(3)	-21(4)	-17(3)	14(3)
O	-211(3)	4341(3)	7064(3)	129(4)	95(5)	113(3)	-5(3)	15(3)	-1(3)
N	-751(4)	6612(4)	7314(3)	112(4)	92(5)	93(3)	1(4)	20(3)	9(3)
C1	1422(5)	5985(6)	7697(4)	112(5)	133(7)	71(3)	-3(5)	13(3)	11(4)
C2	73(4)	5574(5)	7326(3)	118(5)	95(6)	59(3)	4(5)	15(3)	19(3)
C3	-2100(5)	6345(6)	7027(5)	107(6)	131(7)	133(6)	5(5)	39(5)	25(5)
C4	-2638(6)	6723(6)	5969(5)	101(6)	124(7)	119(5)	-15(5)	6(4)	-17(5)
CMe1	428(7)	7535(15)	5047(6)	113(7)	504(25)	77(5)	-3(11)	-2(5)	30(10)
CMe2	4563(7)	8270(14)	7499(9)	130(8)	370(22)	143(9)	-36(11)	-8(6)	-107(12)
CMe3	-3123(10)	8626(12)	4856(7)	217(12)	290(18)	109(7)	-49(12)	-27(8)	50(9)
H1C1	154(4)	709(6)	778(4)						
H2C1	175(4)	539(5)	830(4)						
H1C3	-250(4)	703(5)	756(4)						
H2C3	-228(4)	532(6)	710(3)						
H1C4	-338(5)	643(6)	587(4)						
H2C4	-216(5)	613(6)	558(3)						
H1Me1	-30(14)	830(14)	497(11)						
H2Me1	10(11)	652(14)	539(9)						
H3Me1	87(12)	741(13)	441(9)						
H4Me1	70(12)	678(12)	452(11)						
H5Me1	-50(10)	762(12)	539(8)						
H6Me1	15(13)	812(13)	456(10)						
H1Me2	479(10)	938(12)	760(9)						
H2Me2	454(11)	788(15)	825(11)						
H3Me2	505(10)	761(14)	719(9)						
H4Me2	460(10)	711(12)	766(8)						
H5Me2	461(11)	881(15)	807(10)						
H6Me2	505(10)	842(13)	683(8)						
H1Me3	-321(10)	1014(12)	489(8)						
H2Me3	-426(10)	810(12)	487(7)						
H3Me3	-238(9)	801(10)	437(7)						
H4Me3	-328(11)	788(12)	425(9)						
H5Me3	-387(13)	903(15)	499(9)						
H6Me3	-283(10)	927(13)	459(8)						
H	-47(5)	747(6)	747(4)						

[a] The positional parameters for all non-hydrogen atoms are presented in fractional unit cell coordinates (x 10^4). Positional parameters for hydrogen atoms are (x 10^3). Atoms H1Me1 through H6Me3 have been assigned half multiplicity.

[b] The β_{ij} are defined by: $T = \exp[-(h^2\beta_{11} + k^2\beta_{22} + \ell^2\beta_{33} + 2hk\beta_{12} + 2h\ell\beta_{13} + 2k\ell\beta_{23})]$ and are (x 10^4). An isotropic thermal parameter of 2.5 was assigned for all hydrogen atoms.

[c] In this and succeeding tables, estimated standard deviations are given in parentheses for the least significant figures.

Table 8. Observed and calculated structure factor amplitudes

Figure 4. Stereographic view of amidithion with hydrogen atoms omitted
In this and succeeding drawings 50% probability ellipsoids are depicted

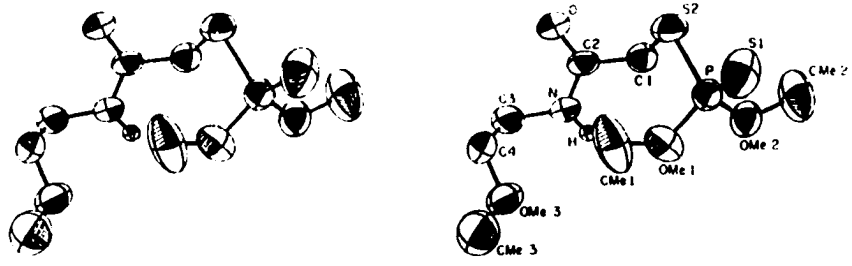
O
S2
C2
C1
S1
CMe 2
P
N
C3
H
C4
OMe 2
CMe 1
OMe 1
OMe 3
CMe 3

Table 9. Bond distances (Å) and angles (°) for amidithion

		Distances	
P-S(1)	1.908(2)	C(3)-C(4)	1.481(9)
P-S(2)	2.050(2)	C(4)-OMe(3)	1.388(6)
P-OMe(1)	1.566(4)	CMe(1)-OMe(1)	1.442(8)
P-OMe(2)	1.562(4)	CMe(2)-OMe(2)	1.429(8)
S(2)-C(1)	1.816(6)	CMe(3)-OMe(3)	1.412(9)
C(1)-C(2)	1.504(7)	P-C(2)	3.910(10)
C(2)-O	1.228(5)	P-H	4.24(2)
C(1)-N	1.323(6)	P-C(3)	5.696(6)
C(3)-N	1.466(7)	P-C(4)	5.805(7)
		Angles	
P-S(2)-C(1)	102.3(2)	P-OMe(2)	121.7(5)
S(1)-P-S(2)	109.0(1)	C(4)-OMe(3)-CMe(3)	112.2(6)
S(1)-P-OMe(1)	118.0(2)	C(2)-N-C(3)	121.7(4)
S(1)-P-OMe(2)	117.6(2)	S(2)-C(1)-C(2)	111.2(4)
S(2)-P-OMe(1)	107.6(2)	C(1)-C(2)-O	120.9(4)
S(2)-P-OMe(2)	108.0(2)	O-C(2)-N	123.3(5)
OMe(1)-P-OMe(2)	95.4(2)	N-C(3)-C(4)	112.4(5)
P-OMe(1)-CMe(1)	120.2(6)	C(3)-C(4)-OMe(3)	109.7(5)

Figure 5. Partial charge densities obtained from CNDO II molecular orbital calculations for amidithion

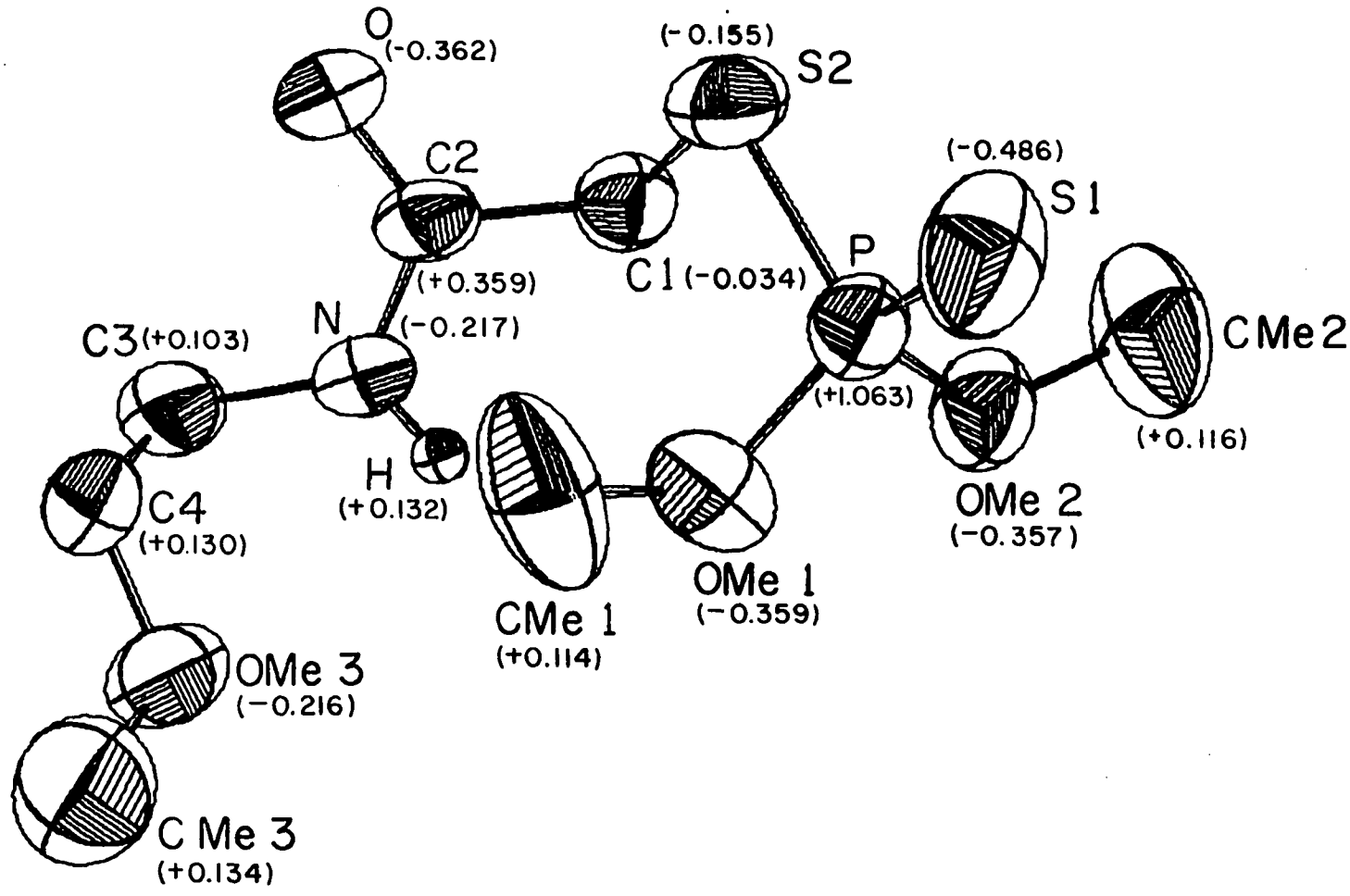
O
(-0.362)
(-0.155)
S2
C2
(-0.486)
S1
C1 (-0.034)
P
(+0.359)
N
(-0.217)
C3 (+0.103)
CMe2
(+1.063)
(+0.116)
H
(+0.132)
C4
(+0.130)
OMe 2
(-0.357)
CMe 1
(+0.114)
OMe 1
(-0.359)
OMe 3
(-0.216)
C Me 3
(+0.134)

the P-C(3) and P-C(4) distances are 5.696(6) and 5.805(7) Å, respectively, although these are less likely candidates for enzyme binding. The P-C(2) and P-H distances are both significantly shorter than the corresponding solid-state separation observed in azinphos-methyl (4.83(2) Å). When autotoxicosis through inhibition of acetylcholinesterase (AChE) by organophosphorus insecticides is considered, it is useful to recall that the nitrogen to carbonyl carbon distance in acetylcholine is estimated at 4.7 Å,[3] when the molecule is in a proper configuration to react with bovine erythrocyte AChE. From a series of experiments carried out by Hollingworth et al.,[4] however, it was concluded that the distance between the anionic and esteratic centers of fly head AChE may be as much as 1 Å greater than that in the mammalian enzyme. In amidithion the primary positive center separations appear to be too small for most efficient binding to the enzyme. Therefore on the basis of configurations found in the solid state, it would appear that amidithion would be less effective than azinphos-methyl in the mammalian systems, assuming that in vivo transport properties are similar and that the inhibition of AChE is the primary toxic mode. Examination of the mammalian LD_{50}'s for azinphos-methyl and amidithion supports this hypothesis, i.e. LD_{50} (azinphos-methyl) = 16, LD_{50} (amidithion) = 420 mg/kg.[5] However we recognize that this distance argument would also suggest that the amidithion molecule would be significantly less effective in insect systems, unless the enzyme interaction with the methylene carbons, C(3) or C(4) are more important than we have assumed.

An examination of intramolecular interactions indicates that the orientation of the phosphate group relative to the rest of the molecule is not necessarily fixed. If one were to allow free rotation about the C(1)-S(2) bond, the molecule could attain maximum positive center separations of approximately 4.7 Å for P-C(2) and 5.5 Å for P-H. However the orientation of the planar segment of the organic moiety would change and its orientation relative to the phosphate group may be important. For example, if one calculates the angle between the normal to the plane of the ring system and the P=O or P=S bond in ronnel,[2] coroxon,[18] and azinphos-methyl,[21] the following results are obtained: 23.67, 38.45, and 23.90°, respectively. In the first two cases in particular, intramolecular interactions tend to dictate these angles and therefore one can assume that they will not change greatly when the moieties are in solution. In amidithion, if one assumes bonding delocalization effects are operative, then C(1), C(2), O, N, and H should define a plane, and indeed the greatest deviation from the least-squares plane defined by these atoms is 0.003 Å. Moreover, for the solid-state configuration found, the angle between this plane and the one normal to the P=S(1) bond is 23.46°, well within the range found in previous studies. If the orientation of the phosphate group relative to the planar segment of the organic moiety is an important topographical factor in the binding of the insecticide to the enzyme, it may be reasonable to assume that the site separations found for amidithion in the solid state are valid parameters in the consideration of effectiveness.

As discussed previously[21] there may also exist a relationship between effectiveness and the partial charge density on the phosphorus atom. The charge on the phosphorus atom of amidithion obtained from CNDO II molecular orbital calculations[20] is +1.063 e (cf. Figure 5). This value is approximately equivalent to that for azinphos-methyl, and consequently, no comparative argument for charge density on phosphorus versus insecticide effectiveness can be made based on these parameters alone.

As noted above, amidithion is approximately twenty-five times less toxic in mammalian systems than is azinphos-methyl. A comparison of solid-state structural features has yielded some supportive evidence to the correlations between effectiveness and positive center separations, and to gross topographical features, particularly if one assumes a preferred orientation of the planar section of the organic moiety relative to the phosphate group. Such a comparison, however, has been inconclusive regarding the importance of partial charge densities. It appears that future structural work should include further investigations as to orientational effects and also the study of an insecticide with an LD_{50} two orders of magnitude greater than azinphos-methyl.

THE CRYSTAL AND MOLECULAR STRUCTURE OF TETRACHLORVINPHOS

Introduction

Previous crystal structure analyses of organophosphorus insecticides have attempted to outline possible structural and electronic features of insecticide molecules which may be important factors when considering their toxicity.[2,18,21,25] As has been discussed, the ubiquitous or specific effectiveness of a particular insecticide may depend on its ability to accommodate a range of esteratic-anionic site separations in various acetylcholinesterase (AChE) enzymes. In addition, the effectiveness may be related to the relative charge densities on the corresponding sites of the insecticide that could be involved in enzyme binding.[21] Finally, gross topographical features of the insecticide molecules may also be important in regulating toxicity.

It is of interest to compare such molecular features among insecticides exhibiting varying degrees of toxic effectiveness. Since our previous studies have included azinphos-methyl, LD_{50} = 16 mg/kg, and amidithion, LD_{50} = 420 mg/kg, we decided to carry out a crystal structural investigation of tetrachlorvinphos, 2-chloro-1-(2,4,5-trichlorophenyl)vinyl dimethylphosphate, $(H_3CO)_2PO_2C_8H_3Cl_4$. It has an LD_{50} of 4000 mg/kg[5] and its structure determination should provide parameters useful for comparison to its more toxic counterparts.

Experimental

Crystal Data A sample of tetrachlorvinphos was kindly supplied by the Pesticides and Toxic Substances Effects Laboratory, U.S.E.P.A., Research Triangle Park, N.C. A nearly spherical crystal of radius 0.18 mm was mounted on a glass fiber with Duco cement and subsequently attached to a standard goniometer head. From five preliminary ω-oscillation photographs taken on an automated four-circle X-ray diffractometer at various χ and ϕ settings, only seven reflections of significant intensity were observed and their coordinates were input to the automatic indexing program ALICE.[6] In spite of the crystal's poor diffraction characteristics, these seven reflections yielded a good cell and intensity data were subsequently collected using this crystal.

The resulting reduced cell and reduced cell scalars indicated a triclinic crystal system. Inspection of the axial ω-oscillation photographs verified, within experimental error, the layer line spacings predicted for this cell by the automatic indexing program. A least-squares refinement of the lattice constants[22] based on the $\pm 2\theta$ measurements of thirteen moderately strong independent reflections on a previously aligned four-circle diffractometer (Mo Kα graphite monochromated X-radiation, λ = 0.70954 Å), yielded a = 14.023(4), b = 15.088(5), c = 6.930(2) Å, α = 93.94(2), β = 90.29(4), and γ = 98.97(4)°.

Collection and Reduction of X-ray Intensity Data Data were collected at room temperature on an automated four-circle diffractometer designed and built in this laboratory. The diffractometer is interfaced to a PDP-15 computer in a time-sharing mode and is equipped with a

scintillation counter. Graphite monochromated Mo Kα X-radiation was used for data collection.

All data within a 2θ sphere of 45° ($(\sin\theta)/\lambda = 0.539\ \text{Å}^{-1}$) in the $hk\ell$, $\bar{h}k\ell$, $h\bar{k}\ell$, and $\bar{h}\bar{k}\ell$ octants were measured via an ω-scan data collection technique, using a take-off angle of 4.5°. There were 3429 reflections measured yielding 1689 independent observed ($|F_o| > 3\sigma_{F_o}$) reflections which were used in subsequent calculations. The relatively rapid decrease in intensity with $\sin\theta/\lambda$ and the relatively small number of observed reflections indicated that some disordering in the solid state might be a strong possibility.

As a general check on electronic and crystal stability, the intensities of six standard reflections were remeasured every 75 reflections. These standard reflections were not observed to vary significantly throughout the entire data collection period. The intensity data were corrected for Lorentz-polarization effects, and since the minimum and maximum transmission factors differed by less than 5% for a nearly spherical crystal with $\mu R = 0.16$, no absorption correction was made.

The estimated variance in each intensity was calculated by

$$\sigma_I^2 = C_T + K_t C_B + (0.03\ C_T)^2 + (0.03\ C_B)^2$$

where C_T, K_t, and C_B represent the total count, a counting time factor, and the background count, respectively, and the factor 0.03 represents an estimate of non-statistical errors. The estimated deviations in the structure factors were calculated by the finite-difference method.[8]

Solution and Refinement

Based on examination of the Howells, Phillips, and Rogers (1950) statistical test for a center of symmetry,[26] the space group was assumed to be $P\bar{1}$. From the volume of the cell (1445 $\AA^3$) it was apparent that there were four molecules per cell, i.e. two molecules per asymmetric unit. Conventional Patterson techniques, as well as the direct methods procedure of Main et al.,[9] proved unsuccessful in elucidating the structure. A direct methods computer program package written by Dr. F. Takusagawa,[27] formerly of this laboratory, was subsequently employed in the solution of the structure. From a list of calculated $|E|$'s, a basis set of nine reflections with large E-values was selected. Three reflections were chosen to define an origin and the signs of the other six were systematically varied. This yielded 64 starting sets as input to the $\Sigma 2$ phase extension algorithm. The starting set yielding the best figures of merit is presented in Table 10. The E-map[10] resulting from the solution set of 418 large $|E|$'s unambiguously revealed the positions of 11 atoms in molecule (A) and 16 atoms in molecule (B). The remaining atoms were found by successive structure factor[11] and electron density map calculations. The positions of the vinyl and phenyl hydrogen atoms were obtained from difference electron density map calculations. The methyl hydrogen positions were approximated by two sets of methyl hydrogens for each methyl carbon atom. The sets were displaced by 60° and were each assigned half-multiplicity.

In addition to positional parameters for all atoms, the anisotropic thermal parameters for all non-hydrogen atoms were refined by a full-matrix

Table 10 . Starting set of E's yielding the best solution

h	k	ℓ	E-value	Sign
5	-2	-5[a]	4.39	+
4	-7	-4[a]	4.34	+
8	7	3[a]	4.06	+
0	1	-6	4.32	-
4	0	0	4.13	-
4	9	3	3.52	-
8	1	0	3.44	-
6	-3	-3	2.93	+
2	4	4	2.77	+

[a]Origin defining reflections

least-squares procedure,[11] minimizing the function $\Sigma\omega(|F_o| - |F_c|)^2$, where $\omega = 1/\sigma^2_{F_o}$, to a conventional discrepancy factor of $R = \Sigma||F_o| - |F_c||/\Sigma|F_o| = 0.138$. Disorder of some of the atoms in one phosphate group, P(A), was evident. In order to partially account for this disorder, extra atoms were included around the phosphorus and occupancy factors of less than unity utilized. Analysis of the weights (ω) was performed via a requirement that $\omega(|F_o| - |F_c|)^2$ should be a constant function of $|F_o|$ and $(\sin\theta)/\lambda$.[12] Such analysis indicated that reflections at high $(\sin\theta)/\lambda$ values were somewhat overweighted, and the weights were subsequently adjusted. No extinction effects were noted. Successive iterations of refinement produced convergence to R = 0.123. The rather high R-value is a direct result of the disordering. The rapid fall-off in intensities with $\sin\theta/\lambda$ is also a manifestation of this disorder. In fact, if only data with $2\theta < 30^o$ are included in the refinement, convergence with R = 0.088 is obtained. The scattering factors used for non-hydrogen atoms were those of Hanson et al.,[13] modified for the real and imaginary parts of anomalous dispersion.[14] The hydrogen scattering factors were those of Stewart et al.[24]

The final positional and thermal parameters are listed in Tables 11, 12, and 13. The standard deviations were calculated from the inverse matrix of the final least-squares cycle. In addition, the multiplicities (occupancy factors) for atoms in the disordered phosphate group of molecule (A) are also given in Table 11. A listing of observed and calculated structure factor amplitudes is provided in Table 14.

Table 11. Final non-hydrogen atom positional parameters ($\times 10^4$) and multiplicities

Atom	Multiplicity	x	y	z
Cℓ(1A)	1.0	667(5)[a]	9114(4)	7008(10)
Cℓ(2A)	1.0	1120(5)	7400(4)	612(8)
Cℓ(3A)	1.0	116(5)	3952(4)	1828(9)
Cℓ(4A)	1.0	1296(5)	4446(4)	6358(9)
P(A)	1.0	3156(4)	8391(4)	5473(10)
O(1A)	0.601	3112(20)	7934(20)	7406(36)
O(2A)	1.0	2126(9)	8381(9)	4560(19)
OMe(1A)	0.644	3552(16)	9418(16)	5560(35)
OMe(2A)	0.568	3730(17)	7929(19)	3955(46)
O(1A')	0.486	3330(22)	7572(24)	6053(47)
OM(1A')	0.351	3235(31)	9148(34)	7299(74)
OM(2A')	0.426	3883(26)	8854(25)	3892(51)
CMe(1A)	0.895	3299(30)	10045(27)	6989(60)
CMe(2A)	1.020	3895(27)	8287(23)	2048(39)
C(1A)	1.0	609(16)	8003(15)	6011(27)
C(2A)	1.0	1382(15)	7784(15)	4977(24)
C(3A)	1.0	1274(12)	6867(13)	4211(25)
C(4A)	1.0	1241(12)	6576(13)	2225(27)
C(5A)	1.0	1160(14)	5713(15)	1529(33)
C(6A)	1.0	1198(16)	5026(14)	2687(30)
C(7A)	1.0	1259(13)	5271(14)	4761(30)
C(8A)	1.0	1337(15)	6191(13)	5479(34)
Cℓ(1B)	1.0	5663(5)	9021(5)	7398(11)
Cℓ(2B)	1.0	6257(5)	7292(5)	13297(9)
Cℓ(3B)	1.0	6424(5)	3894(4)	10945(9)
Cℓ(4B)	1.0	6231(5)	4364(4)	6549(9)
PB	1.0	8123(4)	8374(4)	8927(9)
O(1B)	1.0	8124(12)	7990(11)	6955(19)
O(2B)	1.0	7031(9)	8299(9)	9768(18)
OMe(1B)	1.0	8681(12)	7870(12)	10355(27)
OMe(2B)	1.0	8536(10)	9378(9)	9420(21)
CMe(1B)	1.0	8815(27)	8153(26)	12504(39)
CMe(2B)	1.0	8290(26)	10039(26)	8076(58)
C(1B)	1.0	5571(19)	7917(16)	8027(32)
C(2B)	1.0	6252(15)	7688(13)	9004(27)
C(3B)	1.0	6311(13)	6749(14)	9511(30)
C(4B)	1.0	6331(16)	6493(15)	11416(28)
C(5B)	1.0	6315(15)	5631(13)	11886(30)
C(6B)	1.0	6329(15)	5006(15)	10375(38)
C(7B)	1.0	6253(15)	5188(17)	8394(36)
C(8B)	1.0	6241(17)	6063(17)	8000(38)

[a] in this and succeeding tables, estimated standard deviations are given in parentheses for the least significant figures and M≡Me.

Table 12. Final non-hydrogen atom thermal parameters ($\times 10^4$)[a]

Atom	β_{11}	β_{22}	β_{33}	β_{12}	β_{13}	β_{23}
Cℓ(1A)	95(5)	70(4)	431(22)	13(3)	45(8)	-28(7)
Cℓ(2A)	128(5)	68(4)	220(16)	16(4)	-9(7)	26(6)
Cℓ(3A)	115(5)	58(4)	378(21)	11(3)	27(8)	2(7)
Cℓ(4A)	110(5)	73(4)	314(18)	21(4)	-7(7)	49(7)
PA	70(4)	60(4)	301(18)	7(3)	-8(7)	20(6)
O(1A)	91(16)	81(12)	351(40)	3(10)	9(17)	60(20)
O(2A)	68(9)	58(9)	240(37)	-17(7)	25(15)	31(14)
OMe(1A)	90(14)	70(11)	296(30)	-25(10)	4(16)	58(16)
OMe(2A)	62(12)	64(11)	496(53)	22(10)	6(20)	-90(19)
O(1A')	88(13)	97(11)	229(36)	7(10)	38(16)	109(15)
OM(1A')	85(13)	74(12)	340(50)	12(11)	3(20)	11(19)
OM(2A')	86(14)	74(13)	287(45)	-2(10)	22(18)	-27(18)
CMe(1A)	74(24)	91(28)	436(68)	16(20)	-47(30)	-105(32)
CMe(2A)	106(23)	126(16)	231(88)	48(18)	3(38)	22(34)
C(1A)	67(15)	59(13)	221(56)	4(11)	-5(22)	18(21)
C(2A)	94(18)	75(16)	119(50)	47(13)	27(23)	20(22)
C(3A)	46(12)	71(14)	149(54)	22(10)	29(19)	-8(22)
C(4A)	43(12)	51(12)	263(62)	-1(9)	15(20)	69(23)
C(5A)	63(14)	41(13)	339(68)	-7(10)	63(24)	-26(23)
C(6A)	90(17)	54(14)	305(71)	25(12)	34(16)	50(25)
C(7A)	80(16)	69(15)	239(62)	20(12)	-8(24)	98(25)
C(8A)	59(13)	48(13)	269(61)	-12(10)	43(22)	40(22)
Cℓ(1B)	106(5)	70(4)	473(23)	9(4)	-25(8)	72(8)
Cℓ(2B)	147(6)	77(4)	241(17)	18(4)	45(8)	11(6)
Cℓ(3B)	118(5)	61(4)	373(20)	21(3)	40(8)	46(7)
Cℓ(4B)	115(5)	69(4)	281(17)	15(4)	15(7)	-17(6)
PB	77(5)	65(4)	243(17)	11(3)	-4(7)	15(6)
O(1B)	124(13)	91(11)	156(37)	8(9)	51(16)	-32(15)
O(2B)	62(9)	68(9)	250(38)	16(7)	21(14)	22(14)

[a]The β_{ij} are defined by: $T = \exp\{-(h^2\beta_{11} + k^2\beta_{22} + \ell^2\beta_{33} + 2hk\beta_{12} + 2h\ell\beta_{13} + 2k\ell\beta_{23})\}$.

Table 12 (Continued)

Atom	β_{11}	β_{22}	β_{33}	β_{12}	β_{13}	β_{23}
OMe(1B)	104(12)	79(11)	414(53)	41(9)	-26(20)	-14(15)
OMe(2B)	97(11)	57(9)	269(40)	-18(8)	-6(16)	9(33)
CMe(1B)	140(24)	161(27)	166(66)	21(20)	23(30)	99(31)
CMe(2B)	135(23)	72(17)	432(86)	14(16)	5(34)	30(26)
C(1B)	87(18)	84(17)	279(69)	27(14)	1(27)	-42(22)
C(2B)	61(15)	56(13)	237(60)	-12(11)	26(22)	3(25)
C(3B)	51(13)	65(15)	316(71)	25(11)	-20(23)	-9(21)
C(4B)	115(19)	56(14)	142(54)	11(12)	-28(24)	21(22)
C(5B)	89(16)	50(13)	202(58)	1(11)	61(24)	-2(25)
C(6B)	65(15)	55(14)	354(75)	19(11)	-28(25)	14(23)
C(7B)	66(15)	71(15)	208(58)	14(11)	14(22)	76(29)
C(8B)	95(19)	75(17)	350(78)	26(14)	9(29)	

Table 13. Final hydrogen atom positional parameters (x 10^3)[a]

Atom	Multiplicity	x	y	z
H(1A)	1.0	-1(13)	783(12)	659(26)
H(2A)	1.0	129(12)	545(12)	-18(26)
H(3A)	1.0	112(12)	615(12)	693(27)
H(4A)	0.5	487(32)	853(27)	299(60)
H(5A)	0.5	426(33)	814(26)	181(58)
H(6A)	0.5	316(24)	796(23)	-73(55)
H(7A)	0.5	356(24)	677(23)	-56(51)
H(8A)	0.5	397(26)	892(26)	209(55)
H(9A)	0.5	351(29)	808(24)	19(54)
H(10A)	0.5	421(32)	1000(28)	769(55)
H(11A)	0.5	379(31)	1032(32)	811(59)
H(12A)	0.5	285(33)	1053(29)	656(63)
H(13A)	0.5	274(25)	966(23)	707(49)
H(14A)	0.5	386(31)	958(30)	756(65)
H(15A)	0.5	368(37)	1098(36)	688(70)
H(1B)	1.0	490(13)	769(12)	706(26)
H(2B)	1.0	604(12)	540(12)	1359(27)
H(3B)	1.0	634(12)	606(12)	655(28)
H(4B)	0.5	900(32)	895(25)	1280(66)
H(5B)	0.5	821(25)	863(24)	1370(55)
H(6B)	0.5	938(28)	859(25)	1300(55)
H(7B)	0.5	923(26)	717(24)	1310(51)
H(8B)	0.5	864(27)	733(28)	1337(52)
H(9B)	0.5	896(26)	814(27)	1173(63)
H(10B)	0.5	881(26)	1042(30)	956(70)
H(11B)	0.5	759(25)	1057(25)	855(52)
H(12B)	0.5	914(29)	1005(26)	715(60)
H(13B)	0.5	735(25)	996(24)	702(51)
H(14B)	0.5	844(28)	1096(26)	879(60)
H(15B)	0.5	962(15)	1024(23)	675(49)

[a] An isotropic thermal parameter of 2.5 was assigned to all hydrogen atoms

Table 14. Observed and calculated structure factor amplitudes

Description and Discussion

Selected interatomic distances and angles[16] are listed in Tables 15 and 16, respectively, and they are in favorable agreement with those reported previously in the literature. The presence of two molecules in the asymmetric unit affords an excellent opportunity to evaluate the effects of packing forces on the configurations found for the molecule. As has already been noted, packing forces are different enough to allow disordering of one phosphate group but not the other. However examination of Tables 15 and 16 shows that distances and angles in molecule (A) agree with those found for molecule (B) to 5σ or better. Also the corresponding dihedral angles between various planes in both molecules agree to within 3.4° (Table 17) implying that the equilibrium molecular configuration is relatively unperturbed by solid state effects. Since molecule (B) was less affected by disorder, it will be used as representative of the molecular configuration for the majority of the discussion. A view of the tetrachlorvinphos molecule (B) depicting 50% probability ellipsoids[15] is provided in Figure 6, and a unit cell stereograph containing both molecules (A) and (B) is provided in Figure 7.

The geometry about the phosphorus atom appears to be somewhat distorted from tetrahedral as has been observed in prior crystal structure analyses of organophosphorus insecticides.[2,18,21,25] In particular, the angles involving the doubly-bonded oxygen (O(1)) with the methoxy oxygens (OMe(1) and OMe(2)) are approximately 3° to 10° greater than tetrahedral (cf. Table 16). Reduction of the (methoxy-oxygen)-phosphorus-(methoxy-oxygen) angle, however, is to 105(2)°, compared to 95.4(2)° for

Table 15. Interatomic distances (Å) for tetrachlorvinphos

		Molecule (A)	
Cℓ(1A)-C(1A)	1.76(2)	OM(1A')-CMe(1A)	1.37(6)
Cℓ(2A)-C(4A)	1.74(2)	OMe(2A)-CMe(2A)	1.47(4)
Cℓ(3A)-C(6A)	1.67(2)	OM(2A')-CMe(2A)	1.49(4)
Cℓ(4A)-C(7A)	1.73(2)	O(2A)-C(2A)	1.31(2)
PA-O(1A)	1.55(2)	C(1A)-C(2A)	1.37(3)
PA-O(1A')	1.38(3)	C(2A)-C(3A)	1.43(3)
PA-O(2A)	1.57(1)	C(3A)-C(4A)	1.41(2)
PA-OMe(1A)	1.56(2)	C(3A)-C(8A)	1.40(3)
PA-OM(1A')	1.64(5)	C(4A)-C(5A)	1.34(2)
PA-OMe(2A)	1.52(2)	C(5A)-C(6A)	1.36(3)
PA-OM(2A')	1.62(4)	C(6A)-C(7A)	1.46(3)
OMe(1A)-CMe(1A)	1.41(4)	C(7A)-C(8A)	1.43(3)
		Molecule (B)	
Cℓ(1B)-C(1B)	1.74(2)	O(2B)-C(2B)	1.39(2)
Cℓ(2B)-C(4B)	1.73(2)	C(1B)-C(2B)	1.27(3)
Cℓ(3B)-C(6B)	1.77(2)	C(2B)-C(3B)	1.50(3)
Cℓ(4B)-C(7B)	1.72(3)	C(3B)-C(4B)	1.40(3)
PB-O(1B)	1.45(1)	C(3B)-C(8B)	1.41(3)
PB-O(2B)	1.63(1)	C(4B)-C(5B)	1.36(3)
PB-OMe(1B)	1.56(2)	C(5B)-C(6B)	1.36(3)
PB-OMe(2B)	1.55(1)	C(6B)-C(7B)	1.42(3)
OMe(1B)-CMe(1B)	1.52(3)	C(7B)-C(8B)	1.37(3)
OMe(2B)-CMe(2B)	1.49(3)		

Table 16. Bond angles (degrees) for tetrachlorvinphos

Molecule A

O(1A)-PA-O(2A)	112(1)	PA-OM(2A')-CMe(2A)	113(3)
O(1A)-PA-OMe(1A)	117(1)	Cℓ(1A)-C(1A)-H(1A)	91(11)
O(1A)-PA-OM(1A')	70(2)	Cℓ(1A)-C(1A)-C(2A)	118(2)
O(1A)-PA-OMe(2A)	112(2)	O(2A)-C(2A)-C(1A)	123(2)
O(1A)-PA-OM(2A')	144(2)	C(1A)-C(2A)-C(3A)	115(2)
O(1A')-PA-O(2A)	115(1)	C(2A)-C(3A)-C(4A)	126(2)
O(1A')-PA-OMe(1A)	144(2)	C(2A)-C(3A)-C(8A)	119(2)
O(1A')-PA-OM(1A')	111(2)	Cℓ(2A)-C(4A)-C(3A)	116(1)
O(1A')-PA-OMe(2A)	69(2)	Cℓ(2A)-C(4A)-C(5A)	119(2)
O(1A')-PA-OM(2A')	116(2)	C(3A)-C(4A)-C(5A)	125(2)
O(2A)-PA-OMe(1A)	100(1)	H(2A)-C(5A)-C(4A)	126(8)
O(2A)-PA-OM(1A')	105(2)	H(2A)-C(5A)-C(6A)	109(8)
O(2A)-PA-OMe(2A)	106(1)	C(4A)-C(5A)-C(6A)	123(2)
O(2A)-PA-OM(2A')	104(1)	Cℓ(3A)-C(6A)-C(5A)	123(2)
OMe(1A)-PA-OMe(2A)	107(2)	Cℓ(3A)-C(6A)-C(7A)	121(2)
OMe(1A)-PA-OM(2A')	57(1)	C(5A)-C(6A)-C(7A)	116(2)
OM(1A')-PA-OMe(2A)	145(2)	Cℓ(4A)-C(7A)-C(6A)	120(2)
OM(1A')-PA-OM(2A')	104(2)	Cℓ(4A)-C(7A)-C(8A)	120(2)
PA-O(2A)-C(2A)	122(1)	C(6A)-C(7A)-C(8A)	121(2)
PA-OMe(1A)-CMe(1A)	124(2)	H(3A)-C(8A)-C(3A)	130(10)
PA-OM(1A')-CMe(1A)	121(4)	H(3A)-C(8A)-C(7A)	103(10)
PA-OMe(2A)-CMe(2A)	121(2)	C(3A)-C(8A)-C(7A)	121(2)

Molecule B

O(1B)-PB-O(2B)	112(1)	Cℓ(2B)-C(4B)-C(3B)	119(2)
O(1B)-PB-OMe(1B)	112(1)	Cℓ(2B)-C(4B)-C(5B)	117(2)
O(1B)-PB-OMe(2B)	120(1)	C(3B)-C(4B)-C(5B)	124(2)
O(2B)-PB-OMe(1B)	105(1)	H(2B)-C(5B)-C(4B)	120(8)
O(2B)-PB-OMe(2B)	102(1)	H(2B)-C(5B)-C(6B)	121(8)
OMe(1B)-OMe(2B)	104(1)	C(4B)-C(5B)-C(6B)	116(2)
PB-O(2B)-C(2B)	124(1)	Cℓ(3B)-C(6B)-C(5B)	117(2)
PB-OMe(1B)-CMe(1B)	123(2)	Cℓ(3B)-C(6B)-C(7B)	119(2)
PB-OMe(2B)-CMe(2B)	117(2)	C(5B)-C(6B)-C(7B)	124(2)
Cℓ(1B)-C(1B)-H(1B)	93(9)	Cℓ(4B)-C(7B)-C(6B)	122(2)
Cℓ(1B)-C(1B)-C(2B)	119(2)	Cℓ(4B)-C(7B)-C(8B)	121(2)
O(2B)-C(2B)-C(1B)	123(2)	C(6B)-C(7B)-C(8B)	117(2)
C(1B)-C(2B)-C(3B)	125(2)	H(3B)-C(8B)-C(3B)	134(10)
C(2B)-C(3B)-C(4B)	124(2)	H(3B)-C(8B)-C(7B)	104(10)
C(2B)-C(3B)-C(8B)	118(2)	C(3B)-C(8B)-C(7B)	121(2)

Table 17. Configurational similarities of molecules (A) and (B)

Plane	Defined by	Plane	Defined by
1A	O(1A)-PA-O(2A)	1B	O(1B)-PB-O(2B)
2A	O(1A)-PA-OMe(1A)	2B	O(1B)-PB-OMe(1B)
3A	O(1A)-PA-O(2A)-C(2A)	3B	O(1B)-PB-O(2B)-C(2B)
4A	C(3A)-C(5A)-C(7A)	4B	C(3B)-C(5B)-C(7B)

Plane	Plane	Dihedral Angle (degrees)
1A	4A	83.8
1B	4B	84.6
2A	4A	19.7
2B	4B	23.1
3A	4A	72.6
3B	4B	75.5

Torsion Angles

Atom	Atom	Atom	Atom	Bond	Angle (degrees)
PA	O(2A)	C(2A)	C(3A)	O(2A)-C(2A)	74.6
PB	O(2B)	C(2B)	C(3B)	O(2B)-C(2B)	73.4
O(1A)	PA	O(2A)	C(2A)	PA-O(2A)	23.5
O(1B)	PB	O(2B)	C(2B)	PB-O(2B)	20.9

Figure 6. View of tetrachlorvinphos molecule (B) with methyl hydrogen atoms omitted In this and succeeding drawings 50% probability ellipsoids are depicted

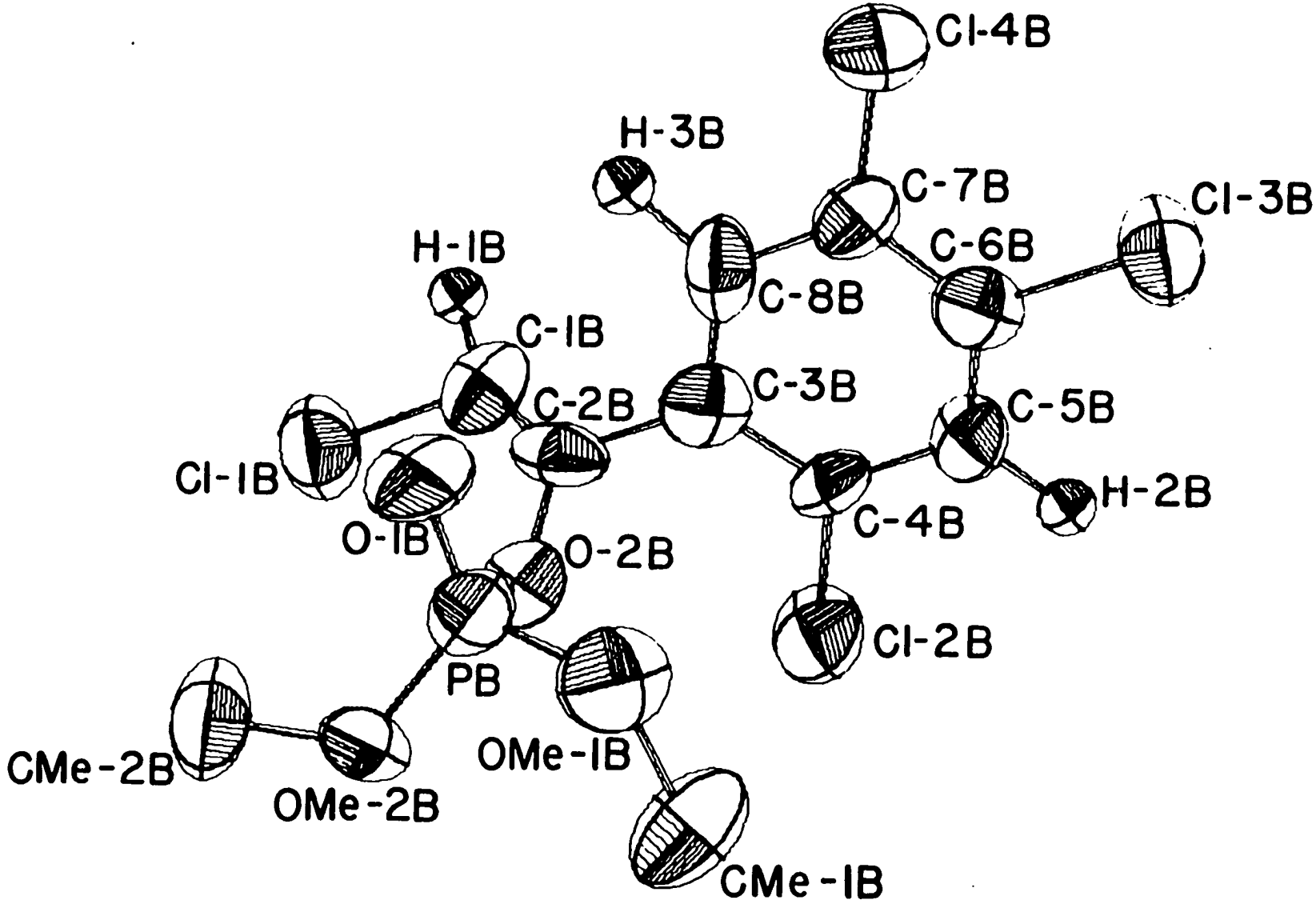
Cl-4B
H-3B
C-7B
Cl-3B
H-1B
C-6B
C-8B
C-1B
C-3B
C-2B
C-5B
Cl-1B
H-2B
C-4B
O-1B
O-2B
Cl-2B
PB
OMe-1B
CMe-2B
OMe-2B
CMe-1B

Figure 7. Unit cell stereograph of tetrachlorvinphos

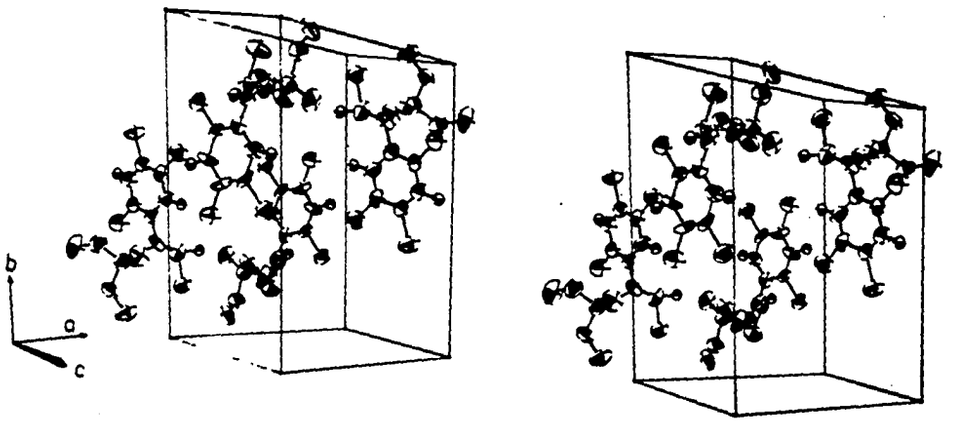
b
a
c

amidithion,[25] 94.3(7)° for azinphos-methyl,[21] and 98.0(3)° for ronnel.[2] The smaller reduction of this angle is due to fewer steric requirements imposed by the doubly-bonded oxygen compared to doubly-bonded sulfur observed in prior studies.

As discussed in the study of amidithion,[25] the orientation of the planar segment of the organic moiety relative to the phosphate group may be an important topographical feature of organophosphorus insecticides. If one calculates the angle between the normal to the plane of the ring system and the P=O bond, the values obtained for tetrachlorvinphos in the solid state configuration are 85.7° for molecule (A) and 85.8° for molecule (B). These results are in poor agreement with 23.7° for ronnel,[2] 39.4° for coroxon,[18] 23.9° for azinphos-methyl,[21] and 23.5° for amidithion.[25] Since both molecule (A) and molecule (B) assume essentially the same configuration, it would appear that this orientation is a preferred one and, therefore, possibly reflects the configuration of the molecule *in vivo* as well. It is tempting to speculate that this apparent deviation in the orientation of the ring system relative to the phosphate group from those of previous studies is correlated to the considerably lower toxicity of tetrachlorvinphos in mammalian systems (LD_{50} = 4000 mg/kg)[5] than the other insecticides mentioned above. The low toxicity could be viewed, in part at least, as due to an inability of this insecticide molecule to accommodate a topographical feature of mammalian AChE enzymes.

When autotoxicosis through inhibition of acetylcholinesterase (AChE) by organophosphorus insecticides is considered, it is useful to recall

that the nitrogen to carbonyl carbon distance in acetylcholine is estimated at 4.7 Å,[3] when the molecule is in a proper configuration to react with bovine erythrocyte AChE. Experiments carried out by Hollingworth et al.,[4] indicated, however, that the distance between the anionic and esteratic centers of fly head AChE may be as much as 1 Å greater than that in the mammalian enzyme. Results of a CNDO II molecular orbital calculation[20] on tetrachlorvinphos indicate that in addition to the phosphorus, there are three probable positive centers that could be involved in enzyme binding (cf. Table 18). They are C(4), C(6), and C(7), and the corresponding distances to the phosphorus are, respectively, 4.1, 5.6, and 5.0 Å for molecule (A), and 4.0, 5.5, and 5.1 Å for molecule (B). It appears that the P-C(4) separations are too small to permit C(4) to be an efficient binding site. C(6) and C(7), however, are far enough away from the phosphorus atom to render them likely candidates for binding to insect and mammalian AChE enzymes, respectively.

Secondary candidates for enzyme binding are H(1), H(2), and H(3) (cf. Table 18). The corresponding phosphorus-hydrogen distances are, respectively, 4.5, 6.0, and 4.2 Å for molecule (A) and 4.6, 6.1, and 4.2 Å for molecule (B). The P-H(3) distances appear to be too short to enable efficient enzyme binding, but H(1) and H(2) could accommodate mammalian and insect AChE enzymes, respectively. Consequently, it is difficult to explain the low mammalian toxicity of tetrachlorvinphos based on positive center separation arguments. The molecule seems to possess a number of positive centers that could accommodate the anionic-

Table 18. Partial charge densities obtained from a CNDO II molecular orbital calculation

Atom	Partial Charge (e)	Atom	Partial Charge (e)
Cℓ(1B)	-0.166	C(1B)	+0.011
Cℓ(2B)	-0.133	C(2B)	+0.188
Cℓ(3B)	-0.145	C(3B)	-0.007
Cℓ(4B)	-0.113	C(4B)	+0.132
PB	+1.385	C(5B)	-0.016
O(1B)	-0.496	C(6B)	+0.127
O(2B)	-0.407	C(7B)	+0.103
OMe(1B)	-0.350	C(8B)	-0.007
OMe(2B)	-0.367	H(1B)	+0.041
CMe(1B)	-0.148	H(2B)	+0.036
CMe(2B)	-0.081	H(3B)	+0.034

esteratic separation requirements of both mammalian and insect AChE enzymes.

As discussed previously,[21] there may exist a relationship between insecticide effectiveness and the partial charge density on the phosphorus atom. The charge on the phosphorus of amidithion[25] is + 1.063 e and that of the phosphorus of azinphos-methyl[21] is + 1.041 e. These two values are not significantly different. It was noted, however, that the charge on phosphorus for the phosphinate analog of azinphos-methyl differs by 0.1 e.[21] The phosphinate analog of azinphos-methyl has an LD_{50} for rats two orders of magnitude larger than azinphos-methyl, i.e. LD_{50} (azinphos-methyl) = 16, LD_{50} (phosphinate analog) ≈ 1000 mg/kg. For tetrachlorvinphos (LD_{50} = 4000 mg/kg), the partial charge on phosphorus is found to be + 1.385 e (cf. Table 18). It is readily apparent that this value is significantly different from the values obtained for either azinphos-methyl or amidithion. If there exists an optimum charge on phosphorus for which enzyme binding or phosphorylation is enhanced, it would appear to be close to the value found for azinphos-methyl. It could then be hypothesized that any deviation from some "optimum" value for the charge on phosphorus would decrease the effectiveness of the insecticide. In order to substantiate or refute this hypothesis, however, further data on additional insecticides is required.

Tetrachlorvinphos is approximately 400 times less toxic in mammalian systems than is azinphos-methyl and is approximately 10 times less effective than amidithion. It is not clear from positive center separation arguments why the former should be less toxic. Topographical

features may be the primary contributor to the low toxicity as evidenced by the dissimilarity of the orientation of the planar organic moiety relative to the P=O bond for tetrachlorvinphos compared to previously studied insecticides. Another possible factor could be the partial charge density on the phosphorus, which is supported by the significant difference in partial charge observed for tetrachlorvinphos compared to the insecticides examined prior to this work. However, further studies of insecticides are necessary to accumulate correlations between effectiveness and the molecular parameters.

THE CRYSTAL AND MOLECULAR STRUCTURE OF THE DECACOORDINATE COMPLEX TRIS(BICARBONATO)TETRAAQUOHOLMIUM (III) DIHYDRATE, $Ho(H_2O)_4(HCO_3)_3 \cdot 2H_2O$

Introduction

Lanthanide chemistry has attracted a great deal of interest recently, due, in no small part, to the capability of the lanthanide metal ions to acquire large coordination numbers. Of considerable interest, then, is the preferred ground state geometries of some of the higher coordination schemes. As discussed by Muetterties and Wright[28] and by Karraker,[29] there are many factors which govern the formation of high coordination compounds. One of these is the size of the metal ion, i.e. the larger the metal ion, the more likely the formation of a species of high coordination number. Another important consideration is the ligand itself and the constraints it places on the system. As is readily apparent, a multi-dentate ligand imposes more steric requirements than does a monodentate ligand. And, finally, ligand-ligand repulsions also dictate the geometry of the system and hence the coordination number.

For ten-coordination, two idealized polyhedra consistent with an sp^3d^5f hybridization scheme are the s-bicapped dodecahedron of D_2 symmetry and the s-bicapped square antiprism of D_{4d} symmetry shown in Figure 8. The similarity of the two polyhedra is demonstrated in Figure 9, in which an s-bicapped square antiprism is distorted sufficiently to produce the s-bicapped dodecahedron. Crystallographic studies of ten-coordinate compounds previously reported in the literature

Figure 8 . Idealized polyhedra for decacoordination

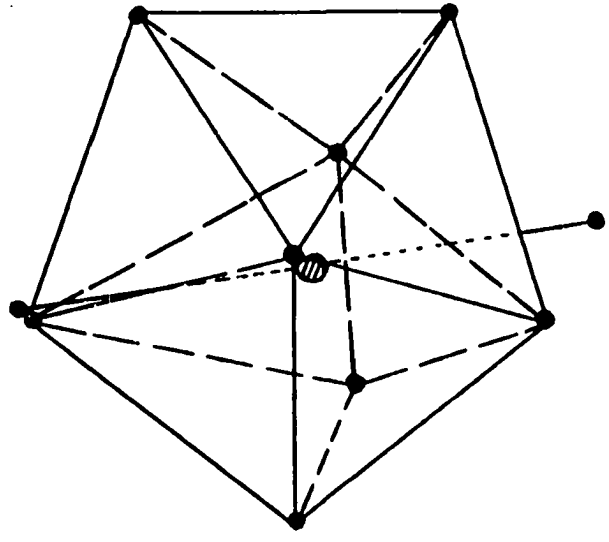

s-bicapped dodecahedron

D_2

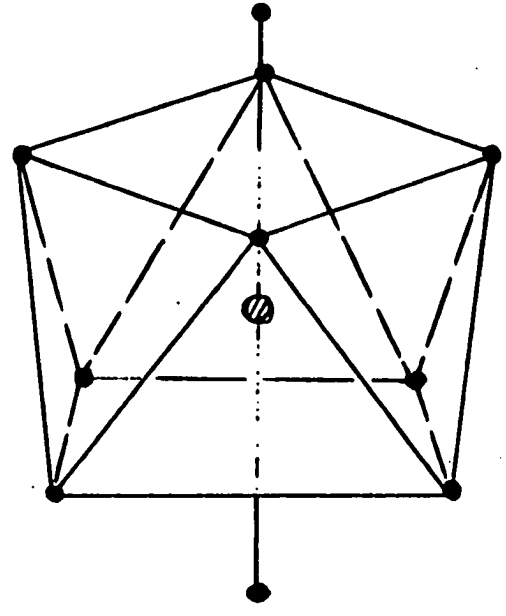

s-bicapped square antiprism

D_{4d}

Figure 9. Formation of dodecahedral geometry via distortion of square antiprism

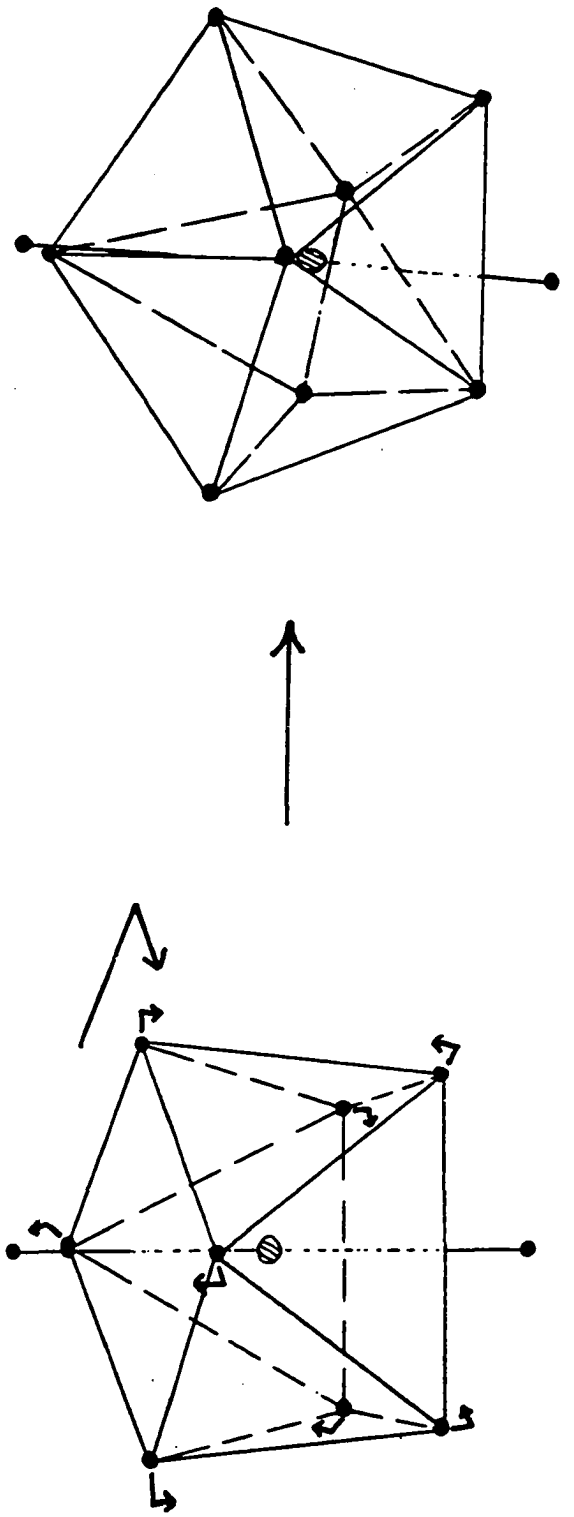

were done on the complexes of the larger lanthanide and actinide metals, e.g. La, Ce, and U. The geometries of such compounds approximate both the s-bicapped dodecahedron[30,31,32] and the s-bicapped square antiprism.[33,34]

In order to determine unequivocally the preferred ground state geometry for ten-coordination, a compound composed of very small, identical, non-interacting, monodentate ligands surrounding the metal ion in an isolated environment would be required. In the absence of such idealized compounds, one must examine the structures of ten-coordinate compounds involving a small metal ion bound to the same type of atoms, e.g. oxygen, with the least amount of constraints imposed by the smallest number of bidentate ligands possible. Having the smallest possible number of bidentate ligands thus introduces the fewest geometrical restrictions on the system, and if the bidentate ligands are small, the ligand-ligand repulsions should be reduced. In addition, using a small lanthanide metal ion instead of one of the larger ones implies that the more stable configuration would predominate, since reducing the size of the coordination sphere increases strain on the high coordination system due to ligand repulsions. Therefore, a sample of tris(bicarbonato) tetraaquoholmium (III) dihydrate ($Ho(H_2O)_4(HCO_3)_3 \cdot 2H_2O$) was prepared for three-dimensional X-ray analysis.

Experimental

Preparation The holmium bicarbonate compound can be prepared in several ways. The two methods employed in this laboratory will be

presented here. Starting with an aqueous 1M $HoCl_3 \cdot 6H_2O$ solution, the holmium carbonate was produced by adding Na_2CO_3 to the solution and filtering off the carbonate precipitate. Then by acidifying the carbonate, a bicarbonate was produced and the acid-H_2O azeotrope was boiled off. Slow evaporation of the bicarbonate solution yielded crystals of varying degrees of hydration. A greater yield of the title compound was realized from a rather novel preparation scheme. A 1M $HoCl_3 \cdot 6H_2O$ solution of pH 3 was added to a saturated aqueous solution of sucrose ($C_{12}H_{22}O_{11}$). The resulting acidic solution was heated sufficiently to boil off the HCl-H_2O azeotrope (108.6°C), and then additional heating was employed to eliminate the excess water. Gradual degradation of sucrose to bicarbonate in the acidic solution coupled with slow evaporation yielded soft light-orange prismatic crystals suitable for X-ray analysis.

Crystal Data A nearly spherical crystal of dimension 0.2 mm. was mounted on the end of a glass fiber with Duco cement, and was coated with a thin layer of commercial nail polish to isolate it from the atmosphere. From preliminary precession photographs, it was apparent that the compound crystallized in the triclinic crystal system. A least-squares refinement[7] of the six lattice constants based on the $\pm 2\theta$ measurements of thirteen strong reflections determined by left-right, top-bottom beam splitting on a previously aligned four-circle diffractometer (Mo Kα radiation, $\lambda = 0.71069$ Å), at 25°C, yielded $\underline{a} = 9.18 \pm .02$, $\underline{b} = 11.59 \pm .01$, $\underline{c} = 6.73 \pm .01$ Å, $\alpha = 88.87 \pm .06$, $\beta = 112.45 \pm .08$, and $\gamma = 71.54 \pm .06°$. A calculated density of 2.44 g/cc for two molecules per unit cell is in good agreement with the observed density of 2.40 ± .05 g/cc, determined

by the flotation method.

Collection and Reduction of X-ray Intensity Data Data were collected at room temperature using an automated four-circle diffractometer designed and built in the Ames Laboratory. The upper full circle was purchased from STOE and is equipped with encoders (Baldwin Optical) and drive motors. The design of the base allows the encoders to be directly connected to the main θ and 2θ shafts, using solid and hollow shaft encoders, respectively. The diffractometer is interfaced to a PDP-15 computer in a real-time mode and is equipped with a scintillation counter. Zirconium-filtered Mo Kα radiation was used for data collection. A scan rate of 0.1 second per step of 0.01° in θ was employed with a variable scan range of 35 steps plus 1 step per degree theta. Stationary-crystal, stationary-counter background counts of a quarter of the scan time were taken at the beginning and end of each scan. Before each scan a peak height measurement was made and, in order to be scanned, the reflection had to exceed the background by more than six counts. If the reflection met this criterion, the ω setting was adjusted slightly, if necessary, to maximize the peak intensity. Within a two-theta sphere of 45° ($\sin\theta/\lambda = 0.538$ Å^{-1}), all data in the hkl, $\bar{h}$kl, $\bar{h}\bar{k}$l, and h$\bar{k}$l octants were measured in this manner, using a take-off angle of 4.5°. Of the 1761 reflections examined, 1709 met the peak height criterion and were scanned to obtain the integrated intensities.

As a general check on electronic and crystal stability, the intensities of three standard reflections were remeasured every twenty-five reflections. These standard reflections were not observed to vary significantly throughout the entire period of data collection.

The intensity data were corrected for Lorentz-polarization effects and, since the crystal was nearly spherical, the minimum and maximum transmission factors differed by ∿4% for μR = 1.3, and no absorption correction was made. The estimated error in each intensity was calculated by

$$\sigma_I^2 = C_T + 2C_B + (0.03\ C_T)^2 + (0.03\ C_B)^2,$$

where C_T and C_B represent the total count and background count, respectively, and the factor 0.03 represents an estimate of non-statistical errors. The estimated deviations in the structure factors were calculated by the finite difference method.[8] Of the 1709 independent reflections, 1621 were considered observed ($>2\sigma_{F_o}$).

Solution and Refinement

Based on examination of the Howells, Phillips, and Rogers[26] statistical test for a center of symmetry, the space group was assumed to be $P\bar{1}$. The position of the holmium atom was obtained from analysis of a three-dimensional Patterson function. The remaining atoms were found by successive structure factor[11] and electron density map calculations.[10] In addition to positional parameters for all atoms, the anisotropic thermal parameters for all non-hydrogen atoms were refined by a full matrix least-squares procedure,[11] minimizing the function $\Sigma\omega(|F_o| - |F_c|)^2$, where $\omega = 1/\sigma_F^2$, to a final conventional discrepancy factor of $R = \Sigma||F_o| - |F_c||/\Sigma|F_o| = 0.039$. The largest ratio of shift of parameter to standard deviation in the final refinement cycle for non-hydrogen atoms was 0.87, and examination of observed and calculated structure factors revealed no appreciable extinction effects. The scattering factors used

were those of Hanson et al.[13] modified for the real and imaginary parts of anomalous dispersion.[14]

The final positional and thermal parameters are listed in Table 19. The standard deviations were calculated from the inverse matrix of the final least squares cycle. Bond lengths and bond angles are listed in Table 20 and Table 21, respectively. Observed and calculated F's are provided in Table 22.

Description and Discussion

Tris(bicarbonato)tetraaquoholmium (III) dihydrate is ten-coordinate with the holmium atom bound to four water oxygen atoms (average distance = 2.362 Å, cf. Table 20) and six bicarbonate oxygens. Two waters of hydration are associated with each molecule and provide crystalline stability through hydrogen bonding. A stereographic view of the molecule is provided in Figure 10.[15]

The holmium-(bicarbonate oxygen) lengths vary from 2.442(9) to 2.557(9) Å with the exception of one long (2.817(11) Å) distance. The latter distance appears to be dictated by the packing of that particular bicarbonate group around the holmium atom. Generally, the two oxygen atoms within a bicarbonate group which are bound to the metal are at different distances from the central ion. The bicarbonate oxygen to which the hydrogen atom is bound is found to be closer to the metal ion by an average of 0.08 Å (2.442(9) to 2.460(10) Å, compared with 2.515(9) to 2.557(9) Å) excluding the bicarbonate group containing the long Ho-O distance mentioned earlier.

The bidentate nature of the bicarbonate groups is evidenced by the

Table 19. Final atom positional[a] and thermal[b] parameters

Atom	x	y	z	β_{11}	β_{22}	β_{33}	β_{12}	β_{13}	β_{23}
Ho	944(1)[c]	2260(0)	3961(1)	90(1)	38(1)	126(2)	-15(0)	47(1)	-8(1)
Ow1	2566(10)	1787(10)	1880(16)	138(17)	94(9)	202(31)	-29(11)	79(19)	-22(13)
Ow2	649(10)	4271(7)	2605(14)	147(14)	41(6)	270(27)	-31(8)	91(17)	-12(10)
Ow3	-1047(12)	2780(8)	337(15)	166(17)	61(8)	202(25)	-42(9)	6(17)	-7(11)
Ow4	514(11)	454(7)	2712(14)	121(15)	48(7)	234(26)	-24(8)	65(17)	-29(11)
O1	-1384(11)	2006(8)	4616(17)	164(16)	75(9)	350(33)	-37(10)	135(20)	-3(13)
O2	-1570(11)	3863(8)	4160(16)	162(16)	76(8)	411(36)	-30(9)	147(21)	-43(14)
O3	-3531(10)	3459(8)	4722(16)	110(15)	101(9)	360(34)	-15(9)	88(18)	11(14)
O4	1783(11)	3296(7)	7330(14)	182(18)	75(8)	260(28)	-40(9)	100(19)	-41(13)
O5	3592(10)	2610(9)	5988(15)	106(14)	108(10)	250(29)	-17(9)	38(17)	-37(15)
O6	4164(11)	3601(8)	8709(15)	166(16)	99(9)	251(29)	-48(10)	25(19)	-69(14)
O7	3836(12)	143(9)	6056(15)	200(18)	146(11)	202(28)	-79(12)	83(19)	-20(14)
O8	1966(10)	751(7)	7360(13)	132(15)	63(7)	212(24)	-13(9)	59(16)	8(11)
O9	4174(11)	-886(8)	8952(15)	151(16)	90(9)	301(32)	-33(10)	45(19)	23(15)
Ow5	3014(11)	4849(9)	1683(16)	122(15)	79(8)	261(32)	-31(9)	31(18)	-14(13)
Ow6	2782(11)	-1345(8)	1869(16)	137(16)	78(8)	185(26)	-30(9)	13(16)	-31(12)
C1	-2207(11)	3123(9)	4507(16)	44(16)	47(10)	103(28)	6(10)	27(17)	3(12)
C2	3220(12)	3187(9)	7391(18)	73(18)	32(8)	158(33)	13(10)	28(21)	1(14)
C3	3357(11)	-18(8)	7476(14)	66(16)	31(8)	33(24)	-4(10)	0(17)	27(12)
Hw1	206(22)	214(16)	18(34)						
H'w1	326(25)	155(21)	250(40)						
Hw2	167(22)	458(16)	250(30)						
H'w2	-24(23)	505(17)	277(29)						
Hw3	-153(24)	237(18)	-29(34)						
H'w3	-189(24)	338(19)	30(32)						
Hw4	130(23)	-30(17)	287(31)						
H'w4	-61(26)	22(18)	269(34)						
H1	-201(22)	194(16)	304(32)						
H2	394(22)	317(17)	529(33)						
H3	98(22)	33(16)	740(29)						
Hw5	373(24)	495(18)	247(35)						
H'w5	329(24)	428(18)	92(33)						
Hw6	389(24)	-176(17)	411(34)						
H'w6	280(24)	-115(18)	101(36)						

[a] The positional parameters for all non-hydrogen atoms are presented in fractional unit cell coordinates (x 10^4). Positional parameters for hydrogen atoms are (x 10^3).

[b] The β_{ij} are defined by: $T = \exp\{-(h^2\beta_{11} + k^2\beta_{22} + l^2\beta_{33} + 2hk\beta_{12} + 2hl\beta_{13} + 2kl\beta_{23})\}$. For all hydrogen atoms an isotropic thermal parameter of 4.5 was assigned.

[c] In this and succeeding tables, estimated standard deviations are given in parentheses for the least significant figures.

Table 20. Selected interatomic distances (Å) for $Ho(H_2O)_4(HCO_3)_3 \cdot 2H_2O$

Ho-Ow1	2.364(10)	C3-O8	1.277(12)
Ho-Ow2	2.380(8)	C3-O9	1.215(12)
Ho-Ow3	2.343(10)	Hydrogen Bonding Distances	
Ho-Ow4	2.362(8)	Hw2-Ow5	1.64(19)
Ho-O1	2.442(9)	H'w5-(O6)'	2.01(21)
Ho-O2	2.515(9)	Ow2--Ow5	2.735(13)
Ho-O4	2.557(9)	Ow5--(O6)'	2.824(14)
Ho-O5	2.460(10)	Hw4-Ow6	1.86(20)
Ho-O7	2.817(11)	Ow6-(Hw3)'	1.96(20)
Ho-O8	2.518(9)	Ow4--Ow6	2.684(12)
C1-O1	1.259(13)	Ow6--(Ow3)'	2.735(12)
C1-O2	1.244(13)	O9--(Ow6)'	2.842(14)
C1-O3	1.219(13)	(H'w6)'-O9	2.27(21)
C2-O4	1.270(13)	Bites of Bicarbonate Groups	
C2-O5	1.257(14)	O1--O2	2.111(12)
C2-O6	1.209(13)	O4--O5	2.131(13)
C3-O7	1.228(13)	O7--O8	2.151(13)

Table 21. Bond angles (degrees) for $Ho(H_2O)_4(HCO_3)_3 \cdot 2H_2O$

Ow1-Ho-Ow2	79.1 (3)	O1-Ho-O4	91.5 (3)
Ow1-Ho-Ow3	75.5 (4)	O1-Ho-O5	138.7 (3)
Ow1-Ho-Ow4	78.1 (4)	O1-Ho-O7	109.0 (3)
Ow1-Ho-O1	146.2 (4)	O1-Ho-O8	68.1 (3)
Ow1-Ho-O2	142.7 (3)	O2-Ho-O4	68.3 (3)
Ow1-Ho-O4	121.8 (3)	O2-Ho-O5	112.9 (3)
Ow1-Ho-O5	72.4 (3)	O2-Ho-O7	147.7 (3)
Ow1-Ho-O7	69.1 (3)	O2-Ho-O8	101.2 (3)
Ow1-Ho-O8	116.0 (3)	O4-Ho-O5	50.2 (3)
Ow2-Ho-Ow3	72.1 (3)	O4-Ho-O7	90.6 (3)
Ow2-Ho-Ow4	140.5 (3)	O4-Ho-O8	69.7 (3)
Ow2-Ho-O1	118.1 (3)	O5-Ho-O7	63.5 (3)
Ow2-Ho-O2	68.9 (3)	O5-Ho-O8	82.3 (3)
Ow2-Ho-O4	75.0 (3)	O7-Ho-O8	47.1 (3)
Ow2-Ho-O5	71.6 (3)	O1-C1-O2	115.0 (9)
Ow2-Ho-O7	130.7 (3)	O1-C1-O3	122.8 (10)
Ow2-Ho-O8	144.4 (3)	O2-C1-O3	122.2 (9)
Ow3-Ho-Ow4	71.2 (3)	O4-C2-O5	115.0 (10)
Ow3-Ho-O1	82.5 (4)	O4-C2-O6	122.4 (11)
Ow3-Ho-O2	76.8 (4)	O5-C2-O6	122.6 (11)
Ow3-Ho-O4	138.6 (3)	O7-C3-O8	118.3 (9)
Ow3-Ho-O5	135.1 (3)	O7-C3-O9	121.2 (10)
Ow3-Ho-O7	130.1 (3)	O8-C3-O9	120.5 (10)
Ow3-Ho-O8	140.9 (3)	H1-O1-C1	97 (10)
Ow4-Ho-O1	70.7 (3)	H5-O5-C2	102 (12)
Ow4-Ho-O2	115.4 (3)	H8-O8-C3	116 (8)
Ow4-Ho-O4	144.3 (3)		
Ow4-Ho-O5	129.5 (3)	Hw4-Ow6-(Hw3)'	103 (8)
Ow4-Ho-O7	68.0 (3)	Hw2-Ow5--(C6)'	125 (6)
Ow4-Ho-O8	75.0 (3)	O9--(Ow6)'-(Hw4)'	132 (5)
O1-Ho-O2	50.4 (3)	O9--(Ow6)'-(Hw3)"	100 (6)

Table 22. Observed and calculated structure factor amplitudes

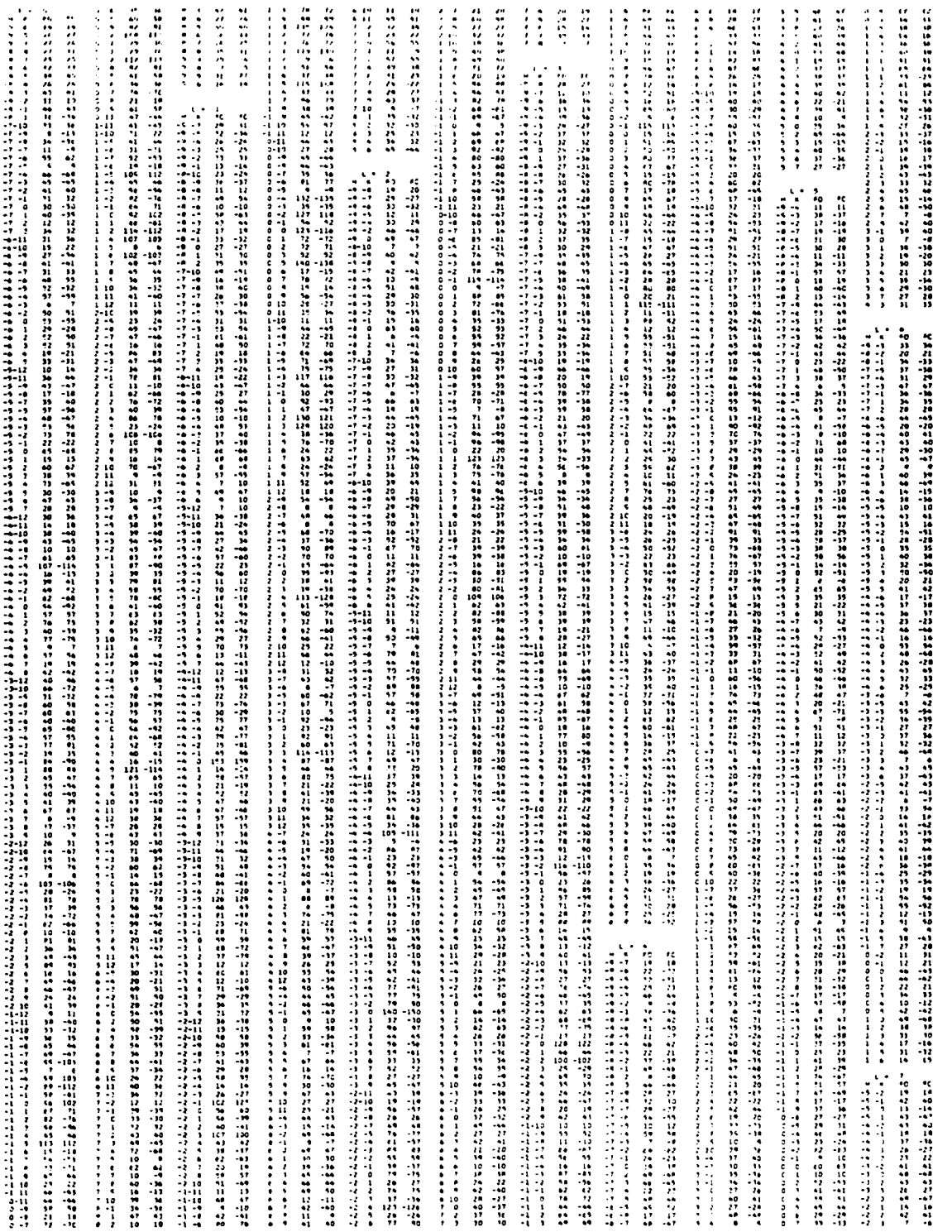

Figure 10. Stereographic view of $Ho(H_2O)_4(HCO_3)_3 \cdot 2H_2O$
In this and succeeding drawings 70% probability ellipsoids are depicted

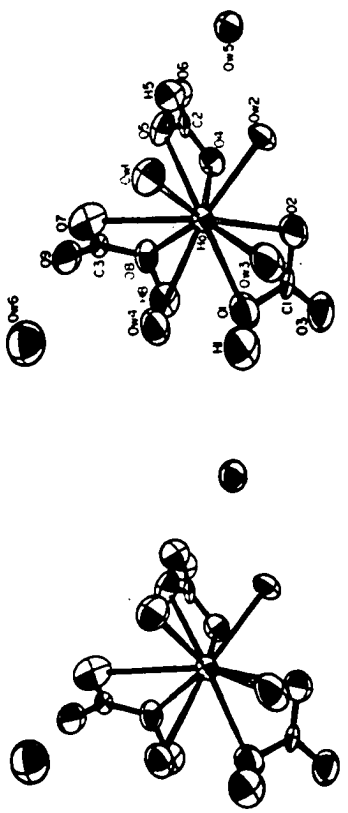
Ow5
H5
O6
C2
O4
Ow2
O7
O2
C3
O8
Ow4
Ow3
Cl1
O3
Ow6
O1
H1

corresponding bites (cf. Table 20) and by the O - C - O angles. As can be seen in Table 21, the metal-bound oxygen-carbon-oxygen angles are significantly smaller than the other oxygen-carbon-oxygen angles in the bicarbonate groups. The bites and angles are consistent with those reported by Shinn and Eick in a paper describing the structure of a ten-coordinate lanthanum compound containing bidentate carbonate groups.[31] It is also apparent that the carbon anisotropic thermal motion in all bicarbonate groups is predominantly out-of-plane motion (cf. Table 19 and Figure 10).

The geometry of $Ho(H_2O)_4(HCO_3)_3 \cdot 2H_2O$ approximates that of the s-bicapped square antiprism more closely than that of the s-bicapped dodecahedron (cf. Figures 8 and 10). Ow1, Ow4, O8, and O5 define one distorted square plane, and Ow2, Ow3, O1, and O4 define the other (see Table 23). The justification for calling the geometry distorted square antiprismatic versus dodecahedral is provided in Table 24, where it is seen that the angles Ow1-Ow4-O8, Ow4-O8-O5, etc., approximate 90° more closely than they do the approximate alternating 77° and 100° consistent with the s-bicapped dodecahedron.[35] In addition, θ_1 corresponding to the Ow1-Ho-O7 type angles averages 58.9° (cf. Table 21), and θ_2 corresponding to O5-Ho-O7 type angles averages 69.2°. The average of θ_1 and θ_2 in this compound is approximately 64.1° which is in good agreement with the energetically favored θ angle of 64.8°[36] consistent with an s-bicapped square antiprism. Having defined the distorted square antiprismatic planes as previously mentioned, the two capping atoms then become O7 and O2.

Table 23. Equations of least-squares planes[a] and dihedral angles

Plane I fitting (Ow2-Ow3-O1-O4):

0.8099 X - 0.5798 Y + 0.0888 Z + 2.7344 = 0

Atom	Distance from Plane (Å)
Ow2	-0.254
Ow3	0.237
O1	-0.178
O4	0.195
Ho	1.024
O2	-1.446

Plane II defined by (Ow2-Ow3-O1):

0.8234 X - 0.4893 Y + 0.2866 Z + 2.2094 = 0

Atom	Distance from Plane (Å)
O4	0.952
O2	-1.132
Ho	1.242

Plane III fitting (Ow1-Ow4-O5-O8):

0.7907 X - 0.5534 Y + 0.2620 Z + 0.0440 = 0

Atom	Distance from Plane (Å)
Ow1	0.145
Ow4	-0.139
O5	-0.132
O8	0.126
Ho	-1.162
O7	1.594

Plane IV defined by (Ow1-Ow4-O8):

0.7346 X - 0.6494 Y + 0.1965 Z + 0.3441 = 0

Atom	Distance from Plane (Å)
O5	-0.555
Ho	-1.289
O7	1.425

Plane V fitting (Ho-Ow1-O7-O8):

0.3200 X + 0.8036 Y + 0.5019 Z - 3.4543 = 0

Atom	Distance from Plane (Å)
Ho	0.048
Ow1	-0.041
O7	0.042
O8	-0.049

Plane VI fitting (Ho-Ow3-O2-O4):

0.3383 X + 0.8727 Y - 0.3520 Z - 1.9254 = 0

Atom	Distance from Plane (Å)
Ho	-0.301
Ow3	0.212
O2	-0.116
O4	0.204

Plane VII fitting (Ho-Ow4-O5-O7):

-0.6388 X - 0.1136 Y + 0.7609 Z - 1.5170 = 0

Atom	Distance from Plane (Å)
Ho	0.170
Ow4	-0.131
O5	-0.130
O7	0.091

Plane VIII fitting (Ho-Ow2-O1-O2):

0.1756 X + 0.2441 Y + 0.9537 Z - 2.8674 = 0

Atom	Distance from Plane (Å)
Ho	0.124
Ow2	-0.112
O1	-0.132
O2	0.120

Dihedral Angles

Plane	Plane	Angle	Plane	Plane	Angle
I	III	169.9°	V	VIII	43.0°
II	IV	168.3°	VI	VII	-54.3°
V	VI	50.7°	VI	VIII	-86.4°
V	VII	85.1°	VII	VIII	54.1°

[a]Planes are defined as $c_1X + c_2Y + c_3Z - d = 0$, where X, Y, and Z are cartesian coordinates which are related to the triclinic cell coordinates (x, y, z) by the transformations:

$$X = xa \sin\gamma + zc\,\{(\cos\beta - \cos\alpha\cos\gamma)/\sin\gamma\},$$

$$Y = xa\cos\gamma + yb + zc\cos\alpha, \quad \text{and}$$

$$Z = zc\left(\frac{\sqrt{1 - \cos^2\alpha - \cos^2\beta - \cos^2\gamma + 2\cos\alpha\cos\beta\cos\gamma}}{\sin\gamma}\right)$$

Table 24. Selected distances (Å) and angles (deg) describing polyhedral geometry

Distances of Interest			
O7--Ow1	2.961(14)	O5--Ow1	2.851(14)
O7--Ow4	2.920(13)	O1--O4	3.578(14)
O7--O5	2.795(14)	O4--Ow2	3.010(13)
O2--Ow2	2.772(13)	Ow2--Ow3	2.781(12)
O2--Ow3	3.020(14)	Ow3--O1	3.155(14)
O2--O4	2.848(13)	Ow1--O8	4.142(14)
Ow1--Ow4	2.978(14)	Ow4--O5	4.361(13)
Ow4--O8	2.972(13)	Ow2--O1	4.135(12)
O8--O5	3.277(13)	Ow3--O4	4.585(14)

Selected Angles			
Ow1-Ow4-O8	88.2(3)	Ow3-O1-O4	85.5(3)
Ow4-O8-O5	88.4(3)	O1-O4-Ow2	77.2(3)
O8-O5-Ow1	84.7(4)	O4-Ow2-Ow3	104.6(3)
O5-Ow1-O4	96.8(4)	Ow2-Ow3-O1	88.1(4)

It is interesting to note that one of the capping atoms, 07, is the one which is involved in the longest Ho-oxygen distance. As can be seen in Table 24, the capping atom-plane atom distances are similar for 07 and 02, thus indicating that if 07 were closer to the holmium atom, ligand-ligand repulsions would decrease stability. To further account for the long (2.817(11) Å) distance between Ho and 07, a close examination of intermolecular interatomic distances is required.

Intermolecular hydrogen bonding through waters of crystallization is depicted in Figure 11, and the corresponding distances are presented in Table 20. In addition, there appears to be a weak, but significant, interaction between the oxygen atom of water-6(Ow6) of an adjacent moiety with 09 of the bicarbonate group containing 07 as shown in Figure 12. The 09---(Ow6)' distance is 2.842(14) Å and the angles of 09-(Ow6)'-(Hw4)' and 09-(Ow6)'-(Hw3)'' average 116° (cf. Tables 20 and 21), thus indicating a hydrogen bond-like interaction. The interaction of 09 with the water of crystallization also affects the spatial positions of the other oxygen atoms within the same bicarbonate group. As seen in Figure 12, the interaction of 09 and (Ow6)' causes 07 to be moved further from the holmium atom, thus producing the long Ho-O bond (2.817(11) Å) observed. Consequently, the coupling of the ligand-ligand repulsions and the hydrogen bond-like interaction with 09 substantiates the fact that the Ho-07 distance is somewhat longer than the other Ho-oxygen distances.

In conclusion, although the bonding of the bicarbonate groups and the holmium atom seems somewhat electrostatic in nature, it should be acknowledged that the molecule does approximate an idealized geometry

Figure 11. Stereographic drawing of the $Ho(H_2O)_4(HCO_3)_3 \cdot 2H_2O$ unit cell and adjacent moieties

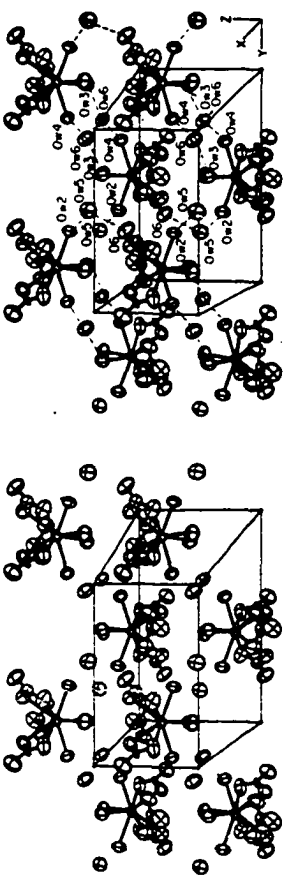

Figure 12. View depicting the O9--(Ow6)' hydrogen bond and the corresponding lengthening of the Ho-O7 distance

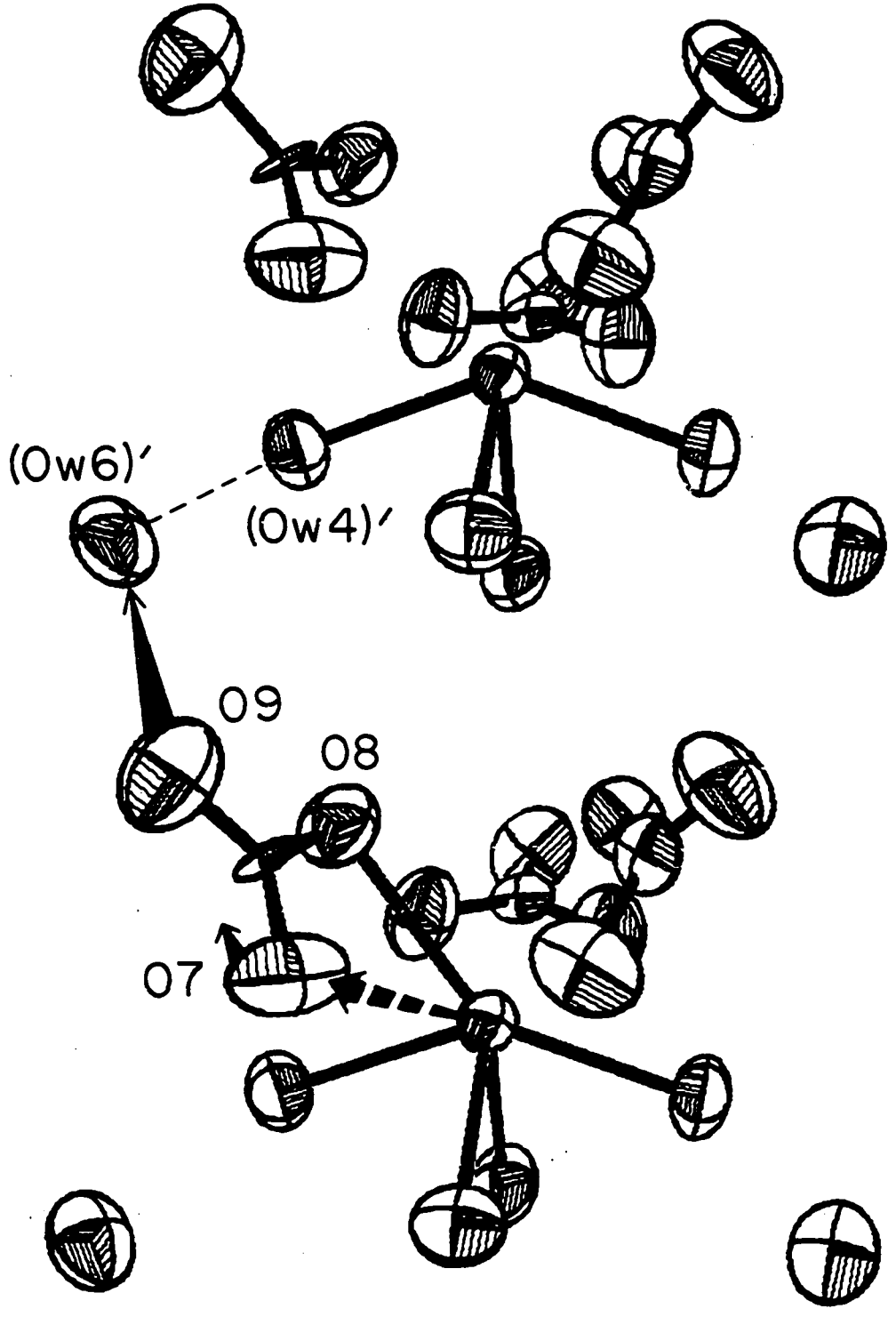
(Ow6)'
(Ow4)'
09
08
07

(bicapped square antiprismatic) rather nicely. Furthermore, since this compound contains the smallest lanthanide ion of any ten-coordinate complex whose three dimensional X-ray analysis has been reported to date, it is conceivable to conclude that the more energetically favored geometry would be more predominant in this compound than in previously reported compounds. Therefore, the structure of tris(bicarbonato) tetraaquoholmium (III) dihydrate supports the results of ligand-ligand repulsion calculations for D_{4d} versus D_2 geometries,[36] which indicate that the D_{4d} (bicapped square antiprismatic) geometry is energetically favored as the preferred ground state geometry for decacoordination.

THE CRYSTAL AND MOLECULAR STRUCTURE OF TRIS(ETHYLENEDIAMINE)-COBALT(III) TETRAKIS (ISOTHIOCYANATO)-COBALTATE(II) NITRATE ($Co^{III}(en)_3Co^{II}(NCS)_4NO_3$)

Introduction

Tris(ethylenediamine)-cobalt(III) tetrakis (isothiocyanato)-cobaltate(II) nitrate ($Co^{III}(en)_3Co^{II}(NCS)_4NO_3$) has been synthesized by Dr. John Bonte in this Laboratory as part of an investigation of solid state isotopic exchange. Substantial isotopic exchange has subsequently been observed for this compound via thermal annealing, and gamma irradiation followed by thermal annealing.[37] In addition, there is considerable interest regarding the polarized absorption spectra of d^3 complexes, i.e. the Co(II) moiety.[38,39] Crystals of $Co^{III}(en)_3Co^{II}(NCS)_4NO_3$ are easily cut for spectral studies to form platelets such that the (0 1 0) face can be mounted perpendicular to the direction of the incident radiation, and such spectral studies are currently underway in this Laboratory.

Detailed molecular and crystal structure information is a necessary prerequisite to comprehensive analysis of the absorption spectra of $Co(NCS)_4^{2-}$, and therefore we embarked on a crystal structure determination of $Co^{III}(en)_3Co^{II}(NCS)_4NO_3$.

Experimental

Crystal Data A crystal of dimensions 0.4 x 0.4 x 0.3 mm was mounted on the end of a glass fiber with Duco cement. From preliminary

ω-oscillation photographs on an automated four-circle diffractometer at various χ and ϕ settings, fourteen moderately strong reflections were selected and input into our automatic indexing program.[6] The resulting reduced cell and reduced cell scalars indicated an orthorhombic crystal system. Orthorhombic mmm symmetry was confirmed by inspection of the three axial ω-oscillation photographs subsequently taken. Observed layer line separations agreed well with those predicted for the cell by the indexing program.

A least-squares refinement of the lattice constants[22] based on the ±2θ measurements of thirteen reflections on a previously aligned four-circle diffractometer (graphite-monochromated Mo Kα radiation, λ = 0.70954 Å) at 25°C, yielded $\underline{a}$ = 10.633(3), $\underline{b}$ = 25.712(6), and $\underline{c}$ = 8.625(2) Å.

Collection and Reduction of X-ray Intensity Data Data were collected at 25°C using an automated four-circle diffractometer designed and built in the Ames Laboratory. The upper full circle was purchased from STOE and is equipped with encoders (Baldwin Optical) and drive motors. The design of the base allows the encoders to be directly connected to the main θ and 2θ shafts, using solid- and hollow-shaft encoders, respectively. The diffractometer is interfaced to a PDP-15 computer in a time-sharing mode and is equipped with a scintillation counter. Graphite-monochromated Mo Kα radiation (λ = 0.70954 Å) was used for data collection. Stationary-crystal, stationary-counter background measurements for 6 seconds were made ±0.5° from the calculated peak center ω value (B_1 and B_2). Scans from peak center in both positive

and negative directions of ω were made in steps of 0.01°, counting for 0.5 seconds at each step until the increment count was less than or equal to the minimum of the backgrounds, after adjustment for counting times. All data (4548 reflections) within a 2θ sphere of 50° ($(\sin\theta)/\lambda = 0.596$) in the $hk\ell$ and $hk\bar{\ell}$ octants were measured in this manner, using a take-off angle of 4.5°.

As a general check on electronic and crystal stability, the intensities of three standard reflections were remeasured every 50 reflections. These standards were not observed to vary significantly throughout the entire data collection period. Examination of the data revealed systematic absences of $h00$, $0k0$, and 00ℓ reflections for $h=2n+1$, $k=2n+1$, and $\ell=2n+1$, respectively, thus defining the space group as $P2_12_12_1$.

The measured intensities were corrected for Lorentz and polarization effects and for absorption[40,41] with minimum and maximum transmission factors of 0.48 and 0.58 ($\mu = 18.25\ cm^{-1}$). The estimated variance in each intensity was calculated by

$$\sigma^2(I) = C_T + K_t\, C_B + (0.03\, C_T)^2 + (0.03\, C_B)^2 + (0.06\, C_N/A)^2$$

where C_T, C_B, C_N, K_t, and A represent the total count, background count, net count, a counting time factor, and the absorption coefficient, respectively. The quadratic terms correspond to the estimated systematic errors in the intensity, background, and absorption correction of 3,3, and 6%, respectively. The standard deviations in the structure factor amplitudes were obtained by the method of finite differences.[8] Reflections for which $Fo > 2\sigma_{Fo}$ (3009 reflections) were used in the refinement

of the two enantiomorphs.

Solution and Refinement

The position of Co(A) was obtained from analysis of a three-dimensional Patterson function. The remaining atoms were found by successive structure factor[11] and electron density map calculations.[10] In addition to positional parameters for all atoms, the anisotropic thermal parameters for all non-hydrogen atoms were refined by a full-matrix least-squares procedure,[11] minimizing the function $\Sigma\omega(|F_o| - |F_c|)^2$, where $\omega = 1/\sigma_F^2$, to a conventional discrepancy index of $R = \Sigma||F_o| - |F_c||/\Sigma|F_o| = 0.085$ for both enantiomorphs. At this point in the refinement it was observed that 21 strong, low-angle reflections appeared to exhibit secondary extinction effects. A plot of I_c/I_o versus i_c for these reflections yielded a straight line with slope (2g) of 3.23×10^{-6}. All data were then corrected for secondary extinction by I_o (corrected) $\tilde{=} I_o(1 + 2gI_c)$.

Analysis of the weights (ω) was performed via a requirement that $\omega(|F_o| - |F_c|)^2$ should be a constant function of $|F_o|$ and $(\sin\theta)/\lambda$.[12] No weight adjustment was deemed necessary. Refinement using the unaveraged data set indicated that the contribution from the imaginary part of the anomalous dispersion correction was completely negligible. Therefore, for the final refinement, reflections in the $hk\ell$ and $hk\bar{\ell}$ octants were then averaged, and the related $(F)_{ave.}$ was calculated as $\{\sum_{i=1}^{N} \sigma_i^2(F)\}^{\frac{1}{2}}/N$, where N is the number of observed reflections for a "unique" reflection to be averaged. There were consequently 1638 independent reflections

used in subsequent calculations. The scattering factors used for non-hydrogen atoms were those of Hanson et al.,[13] modified for the real part of anomalous dispersion (Templeton, 1962).[14] The hydrogen scattering factors used were those of Stewart et al.[24] Final convergence was obtained with R = 0.062.

The final positional and thermal parameters are listed in Table 25. The standard deviations were calculated from the inverse matrix of the final least-squares cycle. Observed and calculated |F|'s are provided in Table 26.

Description and Discussion

A stereographic view of $Co^{III}(en)_3Co^{II}(NCS)_4NO_3$ depicting 50% probability ellipsoids[15] is provided in Figure 13. Interatomic bond distances and angles[16] are listed in Tables 27 and 28, respectively, and are in good agreement with those reported previously in the literature.[12,43] However slight distortions from the idealized octahedral and tetrahedral geometries of the $Co^{(III)}$ and $Co^{(II)}$ moieties are observed.

The Co(A)-N(A) distances of the octahedral moiety range from 1.939(12) to 1.975(11) Å, averaging 1.956 Å, and the N(A)-Co(A)-N(A) angles range from 84.5(4) to 99.8(3)°. It is apparent that the hydrogen atoms bound to N(4A) and N(5A) are involved in hydrogen bonding with the oxygen atoms of the nitrate group, i.e. the H(16)···O(3) distance is 1.56(1) Å and the H(18)···O(2) distance is 1.89(1) Å. In addition, H(17) of N(5A) interacts with S(4B) of the $Co^{(II)}$ moiety, i.e. the H(17)···S(4B) distance is 2.280(6) Å. Similarly, the H(1)···S(2B) distance is 2.446(4) Å, while all other H···S distances exceed 2.65 Å.

Table 25. Final atom positional[a] and thermal[b] parameters

Atom	x	y	z	β_{11}	β_{22}	β_{33}	β_{12}	β_{13}	β_{23}
CoA	8781(2)[c]	6217(1)	4262(2)	60(1)	16(1)	111(2)	1(1)	-1(2)	-2(1)
CoB	3647(2)	6360(1)	9257(2)	109(2)	19(1)	144(3)	1(1)	-1(2)	-2(1)
S1B	7938(4)	7120(2)	8470(5)	111(5)	24(1)	190(7)	-2(2)	-3(5)	-1(2)
S2B	746(4)	7595(2)	7350(5)	87(4)	20(1)	218(8)	1(1)	-1(5)	-1(2)
S3B	3010(4)	6648(2)	14563(5)	91(4)	30(1)	158(7)	-4(2)	13(4)	-5(2)
S4B	3719(6)	4886(2)	6073(8)	223(8)	28(1)	360(15)	33(2)	-141(10)	-43(3)
O1	8428(13)	5920(4)	9443(15)	233(19)	15(2)	269(26)	-14(5)	-52(22)	3(6)
O2	7906(13)	5315(4)	8250(11)	217(13)	22(2)	129(16)	-20(5)	-16(15)	-3(5)
O3	7885(14)	5329(5)	10748(13)	232(20)	32(3)	140(17)	-9(6)	20(19)	-5(6)
N	8262(14)	5523(5)	9481(15)	189(20)	19(2)	150(21)	15(6)	-6(19)	1(6)
N1A	8637(12)	6968(4)	4458(13)	123(14)	18(2)	148(18)	6(5)	-25(16)	-3(5)
N2A	9957(12)	6333(5)	2562(15)	89(12)	20(2)	193(21)	-2(4)	38(13)	-4(6)
N3A	7528(11)	6106(5)	5850(15)	75(11)	26(3)	158(20)	6(4)	12(15)	-2(6)
N4A	7383(11)	6177(5)	2791(15)	92(13)	24(3)	181(21)	3(5)	-30(15)	-15(7)
N5A	9091(10)	5463(4)	4036(15)	73(11)	18(2)	214(23)	4(4)	2(15)	1(6)
N6A	10108(11)	6183(5)	5854(16)	82(12)	23(2)	201(22)	-1(5)	-24(15)	-6(7)
N1B	5346(13)	6635(6)	8944(16)	111(15)	33(3)	174(24)	-4(6)	11(16)	-10(7)
N2B	2373(15)	6823(5)	8351(15)	172(20)	20(2)	164(23)	11(6)	-10(18)	-2(6)
N3B	3312(13)	6354(5)	11884(16)	119(16)	25(3)	149(30)	3(5)	15(16)	-3(6)
N4B	3613(13)	5712(4)	8134(17)	116(15)	17(2)	242(26)	-7(5)	15(18)	-5(6)
C1A	9659(16)	7232(5)	3459(18)	140(21)	15(2)	170(24)	-1(6)	9(20)	3(7)
C2A	9791(16)	6906(6)	2036(20)	131(20)	22(3)	175(25)	-16(7)	20(20)	9(8)
C3A	6230(15)	6181(6)	5259(19)	83(15)	24(3)	216(29)	3(6)	5(20)	9(8)
C4A	6221(13)	5967(6)	3660(21)	51(13)	25(3)	260(31)	-4(6)	43(20)	-7(8)
C5A	9907(19)	5283(7)	5322(23)	206(28)	25(3)	256(38)	31(9)	-97(29)	-11(9)
C6A	10750(16)	5671(6)	5832(25)	108(18)	25(3)	324(41)	-12(6)	-40(26)	31(11)
C1B	6319(15)	6843(6)	8773(17)	93(16)	22(3)	140(22)	-5(6)	3(17)	-10(6)
C2B	1704(14)	7154(6)	7949(17)	99(16)	19(3)	126(20)	-8(5)	17(16)	-5(6)
C3B	3177(13)	6478(6)	12740(20)	59(13)	18(3)	189(26)	-4(5)	-2(17)	4(7)
C4B	3655(16)	5358(6)	7299(22)	122(18)	20(3)	258(33)	8(7)	-52(25)	3(9)
H1	766(11)	712(4)	397(14)						
H2	884(11)	704(4)	580(14)						
H3	930(11)	749(4)	320(14)						
H4	1048(11)	721(4)	450(14)						
H5	1055(12)	701(4)	113(14)						
H6	894(11)	686(4)	131(14)						
H7	1091(11)	627(4)	275(15)						
H8	987(11)	603(4)	154(14)						
H9	747(11)	620(4)	566(14)						
H10	790(12)	569(4)	639(14)						
H11	623(11)	652(4)	510(14)						
H12	541(12)	588(4)	605(14)						
H13	545(12)	625(4)	322(14)						
H14	640(11)	558(4)	404(14)						
H15	731(12)	661(5)	215(14)						
H16	781(11)	578(4)	195(14)						
H17	989(11)	536(4)	294(14)						
H18	825(11)	519(4)	398(14)						
H19	928(11)	518(4)	658(14)						
H20	1029(10)	497(4)	493(15)						
H21	160(10)	558(4)	456(14)						
H22	88(11)	580(4)	703(15)						
H23	1048(11)	652(4)	592(14)						
H24	921(11)	615(4)	668(14)						

[a] The positional parameters for all non-hydrogen atoms are presented in fractional unit cell coordinates (x 10^4). Positional parameters for hydrogen atoms are x 10^3.

[b] The β_{ij} are defined by: $T = \exp[-(h^2\beta_{11} + k^2\beta_{22} + l^2\beta_{33} + 2hk\beta_{12} + 2hl\beta_{13} + 2kl\beta_{23})]$ and are (x 10^4). An isotropic thermal parameter of 2.5 was assigned for all hydrogen atoms.

[c] In this and succeeding tables, estimated standard deviations are given in parentheses for the least significant figures.

Table 26. Observed and calculated structure factor amplitudes

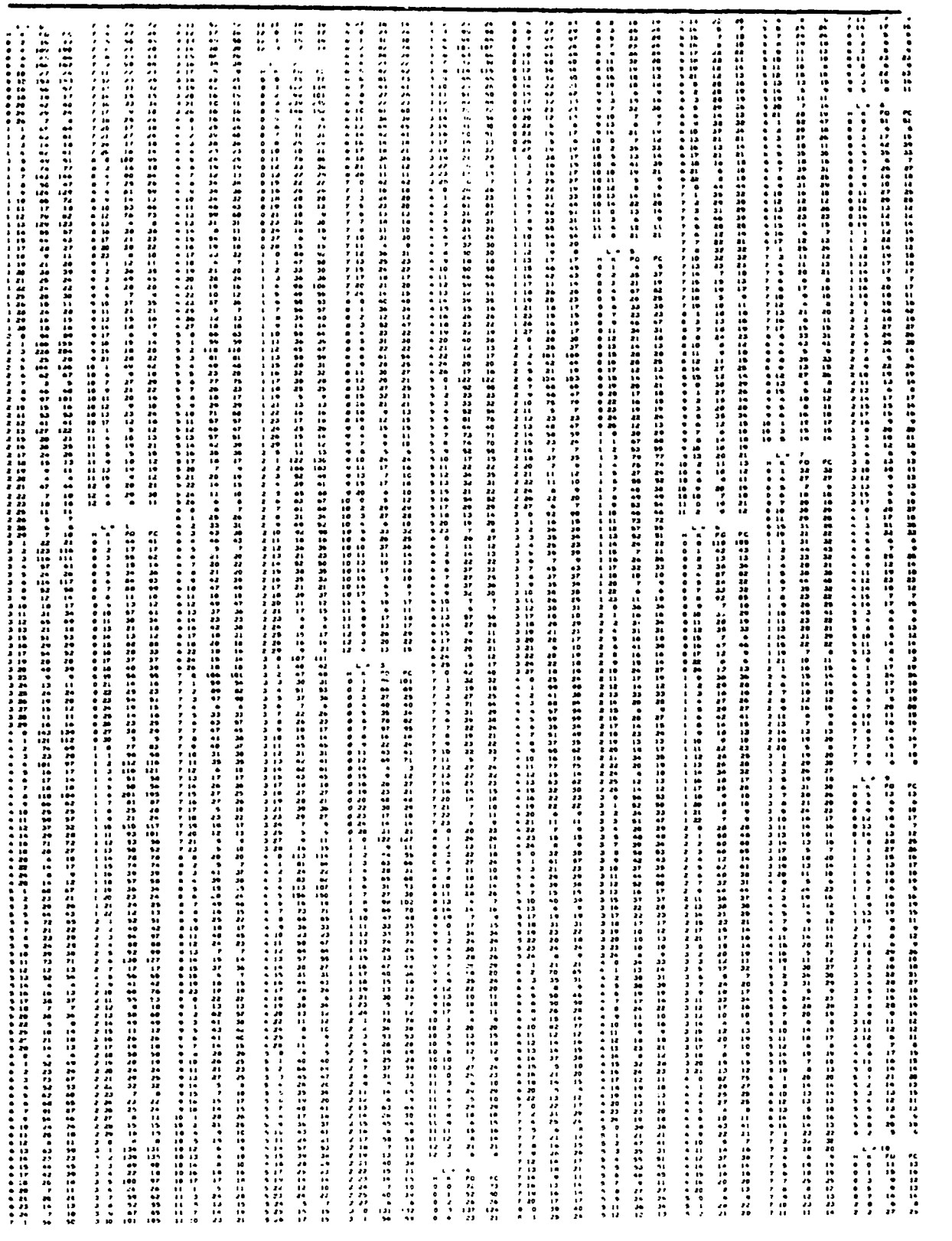

Figure 13. A stereographic view of $Co^{III}(en)_3Co^{II}(NCS)_4NO_3$
In this and succeeding drawings 50% probability ellipsoids are depicted

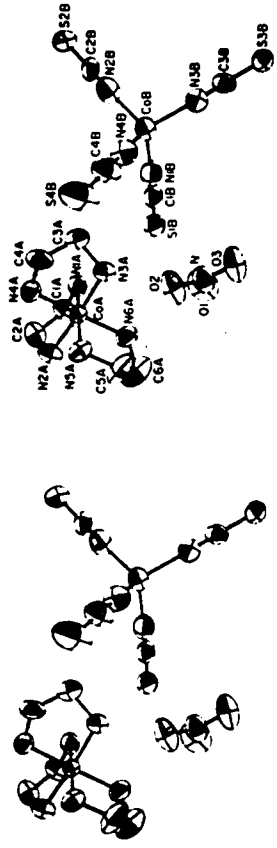
S2B
C2B
N2B
Co1B
N3B
C3B
S3B
C4B
N4B
S4B
C1B N1B
S1B
C4A
C3A
N4A
C1A
N1A
N3A
O2
N
O3
O1
C2A
CoA
N6A
N2A
N5A
C5A
C6A

Table 27. Bond lengths (Å) for $Co^{III}(en)_3Co^{II}(NCS)_4NO_3$

CoA-N1A	1.946(11)	CoB-N1B	1.958(14)
CoA-N2A	1.950(12)	CoB-N2B	1.966(15)
CoA-N3A	1.939(12)	CoB-N3B	1.954(14)
CoA-N4A	1.957(12)	CoB-N4B	1.928(12)
CoA-N5A	1.975(11)	N1B-C1B	1.174(18)
CoA-N6A	1.971(12)	C1B-S1B	1.595(16)
N1A-C1A	1.544(18)	N2B-C2B	1.162(18)
C1A-C2A	1.493(21)	C2B-S2B	1.609(17)
C2A-N2A	1.553(18)	N3B-C3B	1.138(18)
N3A-C3A	1.473(19)	C3B-S3B	1.639(18)
C3A-C4A	1.486(23)	N4B-C4B	1.162(19)
C4A-N4A	1.543(19)	C4B-S4B	1.611(19)
N5A-C5A	1.482(19)	N-01	1.243(17)
C5A-C6A	1.410(23)	N-02	1.248(15)
C6A-N6A	1.483(19)	N-03	1.267(15)

Table 28 . Bond angles (degrees)

N1A-CoA-N2A	84.5(4)	N5A-C5A-C6A	112.7 (15)
N1A-CoA-N3A	91.7(5)	N6A-C6A-C5A	109.8 (14)
N1A-CoA-N4A	92.8(5)		
N1A-CoA-N5A	174.9(5)	N1B-CoB-N2B	111.3(6)
N1A-CoA-N6A	85.3(4)	N1B-CoB-N3B	107.9(6)
N2A-CoA-N3A	176.0(5)	N1B-CoB-N4B	105.1(6)
N2A-CoA-N4A	90.4(5)	N2B-CoB-N3B	105.6(6)
N2A-CoA-N5A	92.4(5)	N2B-CoB-N4B	108.1(6)
N2A-CoA-N6A	94.1(5)	N3B-CoB-N4B	118.9(6)
N3A-CoA-N4A	85.7(5)	CoB-N1B-C1B	173.9 (14)
N3A-CoA-N5A	92.4(5)	CoB-N2B-C2B	169.8 (13)
N3A-CoA-N6A	89.9(5)	CoB-N3B-C3B	163.0 (12)
N4A-CoA-N5A	90.7(5)	CoB-N4B-C4B	171.2 (14)
N4A-CoA-N6A	173.4(5)	N2B-C1B-S1B	177.7 (14)
N5A-CoA-N6A	99.8(3)	N2B-C2B-S2B	177.6 (16)
CoA-N1A-C1A	109.4(8)	N3B-C3B-S3B	178.4 (13)
CoA-N2A-C2A	107.0(9)	N4B-C4B-S4B	177.3 (17)
CoA-N3A-C3A	112.4(10)		
CoA-N4A-C4A	108.1(10)	O1-N-O2	120.2 (13)
CoA-N5A-C5A	109.2(10)	O2-N-O3	121.8 (14)
CoA-N6A-C6A	111.1(10)	O2-N-O3	118.0 (13)
N1A-C1A-C2A	106.2 (12)		
N2A-C2A-C1A	107.7 (12)		
N3A-C3A-C4A	106.2 (12)		
N4A-C4A-C3A	108.4 (12)		

Consequently, the distortions of the octahedral $Co^{(III)}$ and tetrahedral $Co^{(II)}$ groups are manifestations of these hydrogen-bond-like interactions.

The distortions of the tetrahedral $Co^{(II)}$ moiety are evidenced by Co(B)-N(B) distances ranging from 1.928(12) to 1.966(15) Å, averaging 1.952 Å, and by the N(B)-Co(B)-N(B) angles which range from 105.1(6) to 118.9(6)°. In addition, Co(B)-N(B)-C(B) type angles deviate from linearity by as much as 17°.

A unit cell stereograph of the compound is provided in Figure 14,[15] and a stereographic view of the Co(II) species in the unit cell as viewed down the b-axis is provided in Figure 15. From inspection of the dihedral angles between various planes in the $Co(NCS)_4^{-2}$ moiety and the unit cell faces (cf. Table 29), it can be seen that one of the molecular pseudomirror planes is roughly parallel to the bc face; the plane defined by N(3B)-Co(B)-N(4B) subtends an angle of 11.94° with this face.

Table 29. Dihedral angles for the $Co(NCS)_4^{-2}$ moiety

Plane	Crystal Face	Angle (degrees)
N1B-CoB-N2B	ab	25.97
N1B-CoB-N2B	bc	86.25
N1B-CoB-N2B	ac	64.33
N1B-CoB-N3B	ab	80.86
N1B-CoB-N3B	bc	64.75
N1B-CoB-N3B	ac	27.07
N1B-CoB-N4B	ab	38.16
N1B-CoB-N 3	bc	69.80
N1B-CoB-N4B	ac	59.17
N2B-CoB-N3B	ab	87.53
N2B-CoB-N3B	bc	45.66
N2B-CoB-N3B	ac	44.44
N2B-CoB-N4B	ab	53.94
N2B-CoB-N4B	bc	44.65
N2B-CoB-N4B	ac	67.41
N3B-CoB-N4B	ab	79.97
N3B-CoB-N4B	bc	11.94
N3B-CoB-N4B	ac	83.56
N1B-N2B-N3B	ab	67.57
N1B-N2B-N3B	bc	85.43
N1B-N2B-N3B	ac	22.94
N1B-N2B-N4B	ab	13.41
N1B-N2B-N4B	bc	79.64
N1B-N2B-N4B	ac	81.56
N1B-N3B-N4B	ab	64.45
N1B-N3B-N4B	bc	49.71
N1B-N3B-N4B	ac	51.00
N2B-N3B-N4B	ab	81.82
N2B-N3B-N4B	bc	26.47
N2B-N3B-N4B	ac	65.01

Figure 14. Unit cell stereograph of $Co^{III}(en)_3Co^{II}(NCS)_4NO_3$

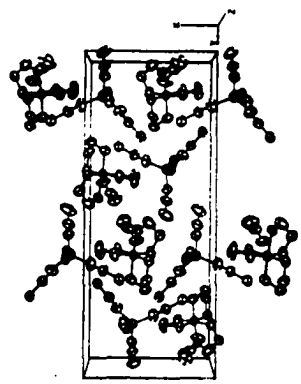

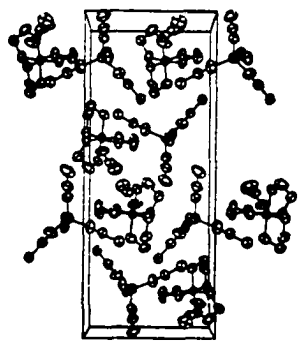

Figure 15. Arrangement of the $Co(NCS)_4^{-2}$ moieties as viewed down the b axis
In this illustration the c axis is vertical

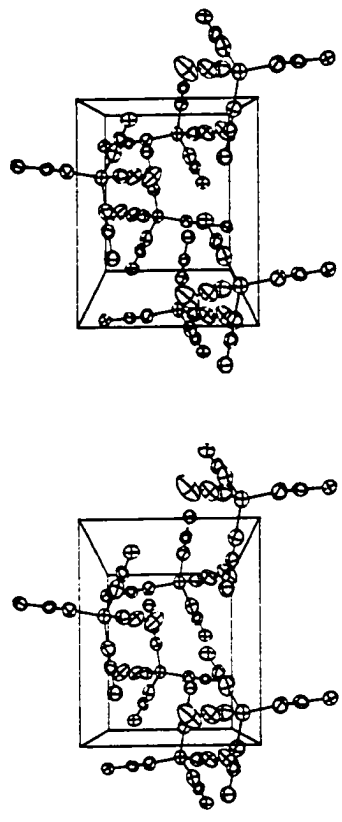

BIBLIOGRAPHY

1. R. D. O'Brien, "Toxic Phosphorus Esters," Academic Press, New York, N.Y., 1960, pp 73-75.

2. R. G. Baughman and R. A. Jacobson, J. Agric. Food Chem., 23, 811 (1975).

3. C. Chothia and P. Pauling, Nature (London), 223, 919 (1969).

4. R. M. Hollingworth, T. R. Fukuto, and R. L. Metcalf, J. Agric. Food Chem., 16, 235 (1967).

5. Pesticides and Toxic Substances Effects Laboratory, "Pesticide Reference Standards and Supplemental Data," National Environmental Research Center, Office of Research and Development, U.S. Environmental Protection Agency, Research Triangle Park, N.C., 1973.

6. R. A. Jacobson, J. Appl. Cryst., 9, 115 (1976).

7. D. E. Williams, "LCR-2, A Fortran Lattice Constant Refinement Program," U.S. Atomic Energy Commission Report IS-1052, Iowa State University and Institute for Atomic Research, Ames, Iowa, 1964.

8. S. L. Lawton and R. A. Jacobson, Inorg. Chem., 7, 2124 (1968).

9. P. M. Main, M. M. Woolfson, and G. Germain, "MULTAN: A Computer Program for the Automatic Determination of Crystal Structures," Department of Physics, University of York, York, England, 1971.

10. C. A. Hubbard, C. O. Quicksall, and R. A. Jacobson, "The Fast Fourier Algorithm and the Programs ALFF, ALFFDP, ALFFPROJ, ALFFT, and FRIEDEL," U.S. Atomic Energy Commission Report IS-2625, Iowa State University and Institute for Atomic Research, Ames, Iowa, 1971.

11. W. R. Busing, K. O. Martin, and H. A. Levy, "ORFLS, A Fortran Crystallographic Least Squares Program," U.S. Atomic Energy Commission Report ORNL-TM-305, Oak Ridge National Laboratory, Oak Ridge, Tennessee, 1962.

12. D. W. J. Cruickshank and D. E. Pilling in "Computing Methods and the Phase Problem in X-ray Crystal Analysis," R. Pepinsky, J. M. Roberts, and J. C. Speakman, Ed., Pergamon Press, New York, N.Y., 1961, pp 45-46.

13. H. P. Hanson, F. Herman, J. D. Lea, and S. Skillman, Acta Crystallogr., 17, 1040 (1960).

14. D. H. Templeton, in "International Tables for X-ray Crystallography," Vol. III, Table 3.3.2c, The Kynoch Press, Birmingham, England, 1962, pp 215-216.

15. C. A. Johnson, "ORTEP-II: A Fortran Thermal-Ellipsoid Plot Program for Crystal Structure Illustrations," U.S. Atomic Energy Commission Report ORNL-3794 (Second Revision with Supplemental Instructions), Oak Ridge National Laboratory, Oak Ridge, Tennessee, 1971.

16. W. R. Busing, K. O. Martin, and H. A. Levy, "ORFFE: A Fortran Crystallographic Function and Error Program," U.S. Atomic Energy Commission Report ORNL-TM-306, Oak Ridge National Laboratory, Oak Ridge, Tennessee, 1964.

17. V. M. Clark, D. W. Hutchinson, A. I. Kirby, and S. G. Warren, Angew. Chem., 76, 704 (1964).

18. M. Gifkins and R. A. Jacobson, J. Agric. Food Chem., 24, 232 (1976).

19. M. Eto, "Organophosphorus Pesticides: Organic and Biological Chemistry," CRC Press, Cleveland, Ohio, 1974, p 275.

20. G. A. Segal, "A Fortran Computer Program Which Calculates Wave Functions and Energies for Molecules in States of any Multiplicity Using the CNDO II Approximation, Modified Version," Carnegie Mellon University, Pittsburgh, Pennsylvania, 1970.

21. W. J. Rohrbaugh, E. K. Meyers, and R. A. Jacobson, J. Agric. Food Chem., 24, 713 (1976).

22. F. Takusagawa, Iowa State University, Ames, Iowa, private communication, 1975.

23. W. J. Rohrbaugh and R. A. Jacobson, Inorg. Chem., 13, 2535 (1974).

24. R. F. Stewart, E. R. Davidson, and W. T. Simpson, J. Chem. Phys., 42, 3175 (1965).

25. W. J. Rohrbaugh and R. A. Jacobson, J. Agric. Food Chem., in press.

26. E. R. Howells, D. C. Phillips, and D. Rogers, Acta Crystallogr., 3, 210 (1950).

27. F. Takusagawa, Iowa State University, Ames, Iowa, private communication, 1976.

28. E. L. Muetterties and C. M. Wright, Quart. Rev. (London), 21, 109 (1967).

29. D. G. Karraker, J. Chem. Ed., 47 (6), 424 (1970).

30. J. L. Hoard, E. Willstadter, and J. V. Silverton, J. Am. Chem. Soc., 87, 1611 (1965).

31. D. B. Shinn and H. A. Eick, Inorg. Chem., 7, 1340 (1968).

32. A. R. Al-Karaghouli and J. S. Wood, Chem. Comm., 1970, 135.

33. I. Jelenic, D. Grdenic, and A. Bezjak, Acta Crystallogr., 17, 758 (1964).

34. R. Wang, R. Bodnar, and H. Steinfink, Inorg. Chem., 5, 1468 (1966).

35. J. L. Hoard and J. V. Silverton, Inorg. Chem., 2, 235 (1963).

36. A. R. Al-Karaghouli and J. S. Wood, Inorg. Chem., 11, 2293 (1972).

37. J. Bonte, Iowa State University, Ames, Iowa, private communication, 1975.

38. T. J. Peters, Iowa State University, Ames, Iowa, private communication, 1976.

39. J. Ferguson, J. Chem. Phys., 39, 116 (1963).

40. J. D. Scott, Queen's University, Kingston, Ontario, Canada, private communication, 1971.

41. J. DeMeulanaer and H. Tompa, Acta Crystallogr., 19, 1014 (1965).

42. F. Mathieu and R. Weiss, J. Chem. Soc., Chem. Comm., 21, 816 (1973).

43. R. J. Balahura, G. Ferguson, and M. L. Schneider, J. Chem. Soc., Dalton Trans., 7, 603 (1975).

ACKNOWLEDGEMENTS

The author wishes to express his appreciation to Dr. R. A. Jacobson for inspiration, guidance, and discussion during the course of this work and to all the members of X-ray Group I for making the graduate educational experience a most enjoyable part of his life. He also wishes to thank S. L. Lawton and Dr. G. T. Kokotailo of Mobil Research and Development Corporation for helping him see the excitement of scientific research. To Brenda Smith, for her conscientious and patient typing of this dissertation, the author owes a special thank you.

In addition, the author wishes to thank his parents whose constant support, moral and financial, have aided him immeasurably during his entire education.

For her understanding, encouragement, sensitivity, and love, the author expresses his deepest appreciation to his wife Phyllis.